Adaptive Fixed Time Nonsingular Terminal Sliding-Mode Control for Quadrotor Formation With Obstacle and Inter-Quadrotor Avoidance

WEI SHANG, GUOHAO JING, DAODE ZHANG, TIANLONG CHEN, AND QIHANG LIANG
School of Mechanical Engineering, Hubei University of Technology, Wuhan 430068, China
Corresponding author: Daode Zhang (hgzdd@126.com)

ABSTRACT In this paper, a robust and safety distributed formation control with unknown external disturbances is researched. For a multi-quadrotors system, a novel nonsingular terminal sliding mode control strategy is studied to realize the formation control with collision avoidance and inter-quadrotor avoidance. The formation controller is redesigned once the system reaches the small field of sliding surface to solve the existence of singular of quadrotor formation and realize the fixed time convergence of singularity region. Then, the position controller and attitude controller are designed to maintain formation configuration with collision avoidance and track the desired angular rate with disturbances, respectively. The global fixed time convergence of quadrotor formation is verified by Lyapunov theory with the fixed time convergence characteristic of singularity region and nonsingular region. At last, simulation results are presented to demonstrate the efficiency of the developed algorithm.

INDEX TERMS Adaptive systems, control theory, systems engineering and theory, sliding mode control, adaptive control, air safety, fixed time convergence, quadrotor formation.

I. INTRODUCTION

In recent decades, the distributed formation control for multi-quadrotors has received considerable attention, which is not only because of the broad applications of quadrotor, such as surveillance, attack, location and observation, but also the reason of the superiority of multi-quadrotors than the single quadrotor, such as better robustness and larger service areas [1], [2]. The communication for each quadrotor uses only the local information to maintain the large number quadrotors into formation configuration and the quadrotor is a typical multi-variable, nonlinear, strong coupled, and underactuated system, which make the formation control a great challenge [3].

In the formation of the quadrotor, due to the obstacles in the environment, which will affect the safety of quadrotor formation and may lead to damage, so formation control with obstacle avoidance is an important issue [4]. An effective way to realize formation safety control of quadrotor is to establish a complete architecture that combines trajectory planner and quadrotor controller [5]. One method is to adopt

the artificial potential field (APF) method [6]–[11], and takes obstacles or other quadrotors as the high potential point. The integrated design of collision avoidance and formation control is realized by using APF function, and the stability of trajectory generation and formation control is proved. In the course of obstacle avoidance, the collision between quadrotors will seriously threaten the formation safety. Therefore, in the process of obstacle avoidance, the distance between quadrotors also needs to be considered. By introducing an APF method, the quadrotor is regarded as a high potential point. When the quadrotor is too close to others, it will generate thrust to keep the distance. At the same time, if the quadrotors are too far apart, it can increase the opposite force to close the distance, so that the quadrotors can keep the formation. In most safety control literature, both asymptotic stability [12] and finite time stability [13]–[17] have been realized. Compared with the above stability characteristics, for the quadrotor formation with high performance [17], the fixed-time stability is more meaningful, because its convergence time is independent of the initial expression. Moreover, in the process of formation flight, external disturbances and model uncertainties are inevitable, always unknown and rapidly changing, which may affect the stability of formation

The associate editor coordinating the review of this manuscript and approving it for publication was Zheng H. Zhu.

system and further improve the difficulty of formation control [18].

Recently, many novel control methods have been proposed for nonlinear system [19]–[23], such as backstepping method [24], [25], output-feedback method [26], [27] and sliding mode control [28]–[30], where sliding mode control is widely used in the quadrotor control field due to its advantages of robustness to disturbance and uncertainty and simplicity of design. Terminal sliding mode(TSM) [31] control exhibits various superior properties such as finite-time convergence and smaller steady-state tracking errors. Compared with TSM, fast terminal sliding mode control (FTSM) [32] makes the errors be stabilized to zero in a shorter time. But due to the existence of terms with negative fractional powers, these control methods have the singularity problem. In order to overcome this problem, a nonsingular terminal sliding mode control(NTSM) [33] and nonsingular fast terminal sliding mode control(NFTSM) [34] have been proposed. Compared with NTSM, the convergence time of NFTSM control is shorter when states far from the origin. However, the time of these non-singular terminal sliding mode controls is not independent of the initial state, which will lengthen the convergence time of the quadrotor formation. A fixed-time nonsingular fast terminal sliding mode control is proposed [35]. Nevertheless, the convergence time to avoid singularity areas is finite, which will prolong the formation convergence time. To solve this problem, a control method proposed in this paper can guarantee the fixed time convergence in singularity areas. Therefore, the quadrotor formation has a global fixed time convergence characteristic.

Motivated by the above observations, this paper investigates a nonsingular fixed time formation control method for quadrotor formation considering the formation safety and disturbances. The main contributions of this paper can be summarized as:

1. Compared with the obstacle avoidance in [6], a novel safety control strategy with obstacle avoidance and inter-quadrotor collision avoidance in fixed time is proposed with unknown bounds of disturbances.

2. Different from the method [35], the scheme proposed in this paper have fixed time convergence in the singularity region, which can guarantee the global fixed time of formation control.

The rest of the paper is organized as follows. In section II, the graph theory, useful lemmas and mathematical model for quadrotor formation are given. The novel safety strategy is proposed in section III and adaptive nonsingular fixed time formation control method is investigated to design the position controller and attitude controller for quadrotor formation. Simulation results and conclusion are given in section IV and section V, respectively.

II. PRELIMINARIES AND PROBLEM STATEMENT
A. PROBLEM FORMULATION AND SYSTEM MODEL
This paper mainly studies the formation control under one leader and n followers. We use a finite index set to mark the
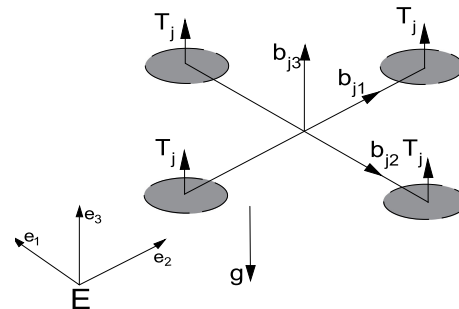

FIGURE 1. Physical structure of a quadrotor.

quadrotor. Mark each following node as $1,2,\ldots,n$, with node index $j \in \Gamma = \{1, 2, \ldots, n\}$, and the leader-quadrotor is a node labeled as zero.

A fixed and undirected graph G is pair (V, ι, A), where $V = (v_1, v_2, \ldots, v_n)$ is note set representing the quadrotor and $\iota = V \times V$ is the edge set. A is the weighted adjacency matrix of G. If there is an edge between agent j and i, then, in other cases. The neighbor set of quadrotor j is denoted as $N_j = \{k : (v_j : v_k) \in \varepsilon\}$. The out-degree of node v_j is defined as $\deg_{out}(v_j) = d_j = \sum_{i=1}^{n} a_{ji} = \sum_{i \in N_j} a_{ji}$. The degree matrix of undirected graph G is $D = diag\{d_1, \ldots, d_n\}$ and the Laplacian matrix of undirected graph G is $L = D - A$. The path from v_i to v_j in graph G is a series of different nodes, starting with v_i and ending with v_j, so that the continuous nodes are adjacent. If there is a path between any two nodes, then graph G is connected. If the jth follower is connected with the leader quadrotor,then $b_j > 0$, in other cases $b_j = 0$. For convenience, set $B = diag\{b_1, \ldots, b_n\}$.

Definition I

Define the function $d_1 : \mathbb{R}^3 \rightarrow \mathbb{R}^3$, the sliding surface is referred to as a fixed-time terminal sliding surface if the following conditions hold

i) $d_1'(\bullet) \neq 0$ for all $y \in R\backslash\{0\}$
ii) $d_1(0) = 0$
iii) $\lim_{y \to 0}(d_1'(\bullet))^{-1} = 0$
iv) $\lim_{y \to 0} \frac{d_1''(\bullet)}{d_1'(\bullet)^3} = \tilde{\gamma} \in \mathbb{R}$

Remark 1: The $d_1(\bullet)$ function can be selected as $d_1(y) = \sqrt{\arctan y}$, which can satisfy the above conditions.

B. PROBLEM FORMULATION
1) QUADROTOR FORMATION MODEL
Fig. 1 shows a basic quadrotor model. Let the subscript "j" $(j = 1, 2, \ldots, n)$ denote the jth quadrotor in the formation, where n is the total number of the quadrotor. The rigid-body dynamic model of the jth quadrotor is as follows:

$$\begin{cases} \dot{p}_j = v_j \\ m_j\dot{v}_j = m_jge_3 - T_jR(Q_j)^T e_3 + d_{Fj} \end{cases} \quad (1)$$

$$\begin{cases} \dot{q}_j = \frac{1}{2}(\eta_jI_3 + S(q_j))\omega_j \\ \dot{\eta}_j = -\frac{1}{2}q_j^T \omega_j \\ I_{fj}\dot{\omega}_j = \Gamma_j - S(\omega_j)I_{fj}\omega_j + d_{\Gamma j} \end{cases} \quad (2)$$
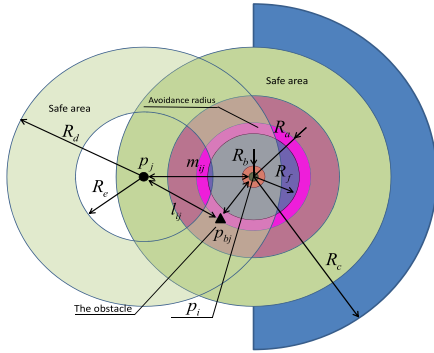
FIGURE 2. Obstacle avoidance model.

where $p_j = \begin{bmatrix} x_j & y_j & z_j \end{bmatrix}^T$ is the position coordinate of the centroid of the quadrotor, and $v_j = \begin{bmatrix} v_{xj} & v_{yj} & v_{yj} \end{bmatrix}^T$ is the velocity of quadrotor in the inertial frame. $Q_j = \begin{bmatrix} q_{j1} & q_{j2} & q_{j3} & \eta_j \end{bmatrix}^T = \begin{bmatrix} q_j^T & \eta_j \end{bmatrix}^T$ is a quaternion used to indicate the direction of quadrotor, which satisfy $q_j^T q_j + \eta_j^2 = 1$. $q_j^T \in \mathbb{R}^3$ is the vector part and $\eta_j \in \mathbb{R}$ is the scalar component. The mass of the jth quadrotor is m_j, and the acceleration component due to gravity is g. $E = \{e_1, e_2, e_3\}$ represents the inertial frame, in which e_3 is the unit vector in the z-axis direction under the inertial system. $B_j = \{b_{j1}, b_{j2}, b_{j3}\}$ represents the body-fixed frame, in which $b_{j3} = [0\ 0\ 1]^T$ is the unit vector in the z-axis direction, T_j is the thrust of the rotor in the b_{j3} direction. The control torque if inner-loop is Γ_j. $I_{fj} = diag(I_{xxj}, I_{yyj}, I_{zzj})$ is the symmetric positive definite constant inertia matrix of the jth quadrotor. $R(Q)$ is the Rodriguez rotation matrix, $R(Q) = (\eta^2 - \|q\|^2)I_3 + 2qq^T - 2\eta S(q)$. d_{Uj} and $d_{\Gamma j}$ are disturbance, which are environment on the quadrotor and the uncertainty of the system model. $S(\bullet)$ is the skew-symmetric matrix operator and defined as

$$S(q) = \begin{bmatrix} 0 & -q_3 & q_2 \\ q_3 & 0 & -q_1 \\ -q_2 & q_1 & 0 \end{bmatrix} \quad (3)$$

The multiplication between quaternions is defined as:

$$Q_1 \odot Q_2 = \begin{pmatrix} \eta_1 q_2 + \eta_2 q_1 + S(q_1)q_2 \\ \eta_1 \eta_2 - q_2^T q_1 \end{pmatrix} \quad (4)$$

where $\odot$ is a non-commutativ multiplication operator.

2) OBSTACLE AVOIDANCE AND INNER-QUADROTOR AVOIDANCE

In this section, obstacle avoidance method and inter-quadrotor collision avoidance method will be introduced. The relevant areas of the jth and ith quadrotors are shown in Fig. 2.

The target avoidance function is defined as

$$\hat{B}(d; (R_{\min}, R_{\max})) = \begin{cases} \dfrac{4(R_{\max}^2 - R_{\min}^2)(R_{\max}^2 - d^2)}{(d^2 - R_{\min}^2)^3}, \\ \quad if d \in (R_{\min}, R_{\max}) \\ 0, \\ \quad otherwise \end{cases} \quad (5)$$

where d is the functional execution area, $R_{\max}$ is the radius at which the function comes into play, $R_{\max}$ is "the threatening radius", which means the quadrotors will avoid the target before this range. The specific effects are shown in detail in section IV.

For the obstacle avoidance, there is $\hat{B}_1 = \hat{B}(l_{jk}; (R_b, R_a))$, where l_{jk} is the distance between obstacle and quadrotor, defined as $l_{jk} = \|p_j - p_{bk}\| (k = 1, 2, \ldots, n)$. p_{bk} is the position of obstacle. Once the jth quadrotor get into the avoidance region $\Psi_a = \{p_j \in \mathbb{R}^3, p_k \in \mathbb{R}^3, \|p_j - p_{bk}\| \in (R_a, R_b)\}$, the quadrotor controller activates the obstacle avoidance function to avoid collision.

For avoid inter-quadrotor collision avoidance, there is $\hat{B}_2 = \hat{B}(m_{ji}; (R_d, R_c))$, where $m_{ji} = \|p_j - p_i\|$ denotes the distance between the jth and ith quadrotor. Once quadrotor jth and ith quadrotor get into the region of $\Psi_b = \{p_i \in \mathbb{R}^3, p_j \in \mathbb{R}^3, \|p_j - p_i\| \in (R_d, R_c)\}$, it means that the distance between the two quadrotors is too close, then the quadrotor will activate the repulsion modes to increase the distance between the quadrotors.

Once jth quadrotor and ith quadrotor get into the region of $\Psi_c = \{p_i \in \mathbb{R}^3, p_j \in \mathbb{R}^3, \|p_j - p_i\| \in (R_f, R_e)\}$ it means that the distance between the two quadrotors is too far, then the quadrotor will activate the attraction module to reduce the distance between the quadrotors. Similarly to the construction of the target avoidance function, the controller will generate a force of magnitude $\hat{B}_3 = \hat{B}(m_{ji}; (R_f, R_e))$.

Remark 2: In this paper, for a quadrotor, the obstacles and neighboring quadrotors are considered as high potential points by using artificial potential approach. When the quadrotor approaches obstacles and other quadrotors, the quadrotor will be pushed away from these objects so as to avoid the obstacles and neighboring quadrotors. Compared with the previous works, the proposed algorithm can make the quadrotor formation reform the preset formation configuration in a global fixed time after avoid obstacles and neighboring quadrotors.

3) CONTROL OBJECTIVE

The main control objective of this article is to make the control law of the quadrotor formation meet the following conditions.

(1) The formation can track desired trajectory and the quadrotor can avoid the obstacle and other quadrotors;

(2) The desired formation configuration can be achieved in global fixed time;

(3) The singularity of the control method can be avoided in the control process of quadrotor formation.

Lemma1 [36]: There exist positive real numbers α and β, positive odd integers m, n, p, q with m > n, p < q such that $\dot{V} \leq -\alpha V^{n/m}(t) - \beta V^{p/q}(t)$. Then, the origin of system is fixed-time stable and the setting time is bounded by

$$t_f < \frac{1}{\alpha} \frac{n}{m-n} + \frac{1}{\beta} \frac{q}{q-p} \quad (6)$$

Assumption 1: The quadrotor's structure is symmetrical and the its propeller structures are rigid.

Assumption 2: The external disturbance d_{Fj} and $d_{\Gamma j}$ are assumed bounded with

$$\left| d_{Fj} \right| < \delta_{Fj}, \left| d_{\Gamma j} \right| < \delta_{\Gamma j}, \quad j = 1, 2, \ldots, n \tag{7}$$

III. MAIN RESULTS

In this section, an adaptive fixed time nonsingular terminal sliding-mode control (AFTNTSC) for quadrotor formation is proposed. The error function and terminal sliding surface are designed for the inner-loop and outer-loop of quadrotor formation. An AFTNTSC control is proposed to so solve the singularity problem. And then, the singularity control law is designed in the singularity region to realize the fixed time convergence of singularity region, so as to guarantee the global fixed time convergence of quadrotor formation.

A. THE OUTER-LOOP SYSTEM STABILITY ANALYSIS

Define the position tracking error as $e_{pj} = \sum_{i=0}^{n} a_{ji}(p_j - p_i - D_{ji})$

and the error of velocity is defined as $e_{vj} = \sum_{i=0}^{n} a_{ji}(v_j - v_i)$.

$\rho_j(t)$ is a sliding surface and defined as:

$$\rho_j(t) = e_{vj} + k_1 e_{pj} \left\| e_{pj} \right\| + k_2 e_{pj} \left\| e_{pj} \right\|^{-\frac{1}{2}} - A^o$$
$$+ \iota_1 \left[\hat{S}(d_1{}'(y)) \right]^{-1} E_1 \tag{8}$$

where $E_1 = [1\ 1\ 1]^T$, $\hat{S}(\bullet) : \mathbb{R}^3 \to \mathbb{R}^{3 \times 3}$ is the diagonal matrix operator and defined as

$$\hat{S}(q) = \begin{bmatrix} q_1 & 0 & 0 \\ 0 & q_2 & 0 \\ 0 & 0 & q_3 \end{bmatrix} \tag{9}$$

A^o denotes the safety function of the quadrotors and defined as

$$A^o = \left[\hat{S}(v_j) \right]^{-1} \sum_{k=1}^{\hat{n}} f_1 \int_0^{\|p_j - p_{bk}\|} \hat{B}_1 l_{jk} d l_{jk} E_1$$
$$+ \left[\hat{S}(v_j - v_i) \right]^{-1} \sum_{i=1}^{n} a_{ji} f_2 \int_0^{\|p_j - p_i\|} \hat{B}_2 m_{ji} d m_{ji} E_1$$
$$- \left[\hat{S}(v_j - v_i) \right]^{-1} \sum_{i=1}^{n} a_{ji} f_3 \int_0^{\|p_j - p_i\|} \hat{B}_3 m_{ji} d m_{ji} E_1 \tag{10}$$

y is a dynamic variable defined as

$$\dot{y} = e_{vj} + k_1 e_{pj} \left\| e_{pj} \right\| + k_2 e_{pj} \left\| e_{pj} \right\|^{-\frac{1}{2}} - A^o \tag{11}$$

Take the time derivative of (8), and submitting (1) to it, there is

$$\dot{\rho}_j(t) = \sum_{i=0}^{n} a_{ji}(g e_3 - \frac{U_j}{m_j} + d_{Uj} - \dot{v}_i) + \beta_1$$
$$+ \dot{A}^o + \iota_1 \left[\hat{S}(d_1{}'(y)) \right]^{-2} \hat{S}(d_1{}''(y)) \dot{y} \tag{12}$$

where

$$\beta_1 = k_1 \left[I + \frac{e_{pj} e_{pj}^T}{\left\| e_{pj} \right\|^2} \right] \left\| e_{pj} \right\| \dot{e}_{pj}$$
$$+ k_2 \left[I - \frac{e_{pj} e_{pj}^T}{2 \left\| e_{pj} \right\|^2} \right] \left\| e_{pj} \right\|^{-\frac{1}{2}} \dot{e}_{pj},$$

$k_1 > 0$, $k_2 > 0$ are constants and

$$\dot{A}^o = - \sum_{k=1}^{\hat{n}} f_1 \hat{B}_1(\|p_j - p_{bk}\|)(p_j - p_{bk})$$
$$+ \frac{\dot{v}_j \sum_{k=1}^{\hat{n}} f_1 \int_0^{\|p_j - p_{bk}\|} \hat{B}_1 l_{jk} d l_{jk}}{v_j^T v_j}$$
$$+ \sum_{i=1}^{n} a_{ji} f_2 \hat{B}_2(\|p_j - p_i\|)(p_j - p_i)$$
$$- \frac{(\dot{v}_j - \dot{v}_i) \sum_{i=1}^{n} a_{ji} f_2 \int_0^{\|p_j - p_i\|} \hat{B}_2 m_{ji} d m_{ji}}{(v_j^T - v_i^T)(v_j - v_i)}$$
$$- \sum_{i=1}^{n} a_{ji} f_3 \hat{B}_3(\|p_j - p_i\|)(p_j - p_i)$$
$$+ \frac{(\dot{v}_j - \dot{v}_i) \sum_{i=1}^{n} a_{ji} f_3 \int_0^{\|p_j - p_i\|} \hat{B}_3 m_{ji} d m_{ji}}{(v_j^T - v_i^T)(v_j - v_i)} \tag{13}$$

To find out the special cases that exist during the sliding process, let

$$\dot{\rho}_j(t) = r_{or}(t) + \beta_1 + \sum_{i=0}^{n} a_{ji} \frac{U_j}{m}$$
$$- \sum_{k=1}^{\hat{n}} f_1 \hat{B}_1(\|p_j - p_{bk}\|)(p_j - p_{bk})$$
$$+ \sum_{i=1}^{n} a_{ji} f_2 \hat{B}_2(\|p_j - p_i\|)(p_j - p_i)$$
$$- \sum_{i=1}^{n} a_{ji} f_3 \hat{B}_3(\|p_j - p_i\|)(p_j - p_i)$$
$$+ \iota_1 \left[\hat{S}(d_1{}'(y)) \right]^{-2} \hat{S}(d_1{}''(y)) \dot{y} \tag{14}$$

where $r_{or}(t)$ is a continuous and twice differentiable term and defined as

$$r_{or}(t) = \sum_{k=0}^{n} a_{jk}(g e_3 + d_{Uj} - \dot{v}_k)$$
$$+ \frac{\dot{v}_j \sum_{k=1}^{n} f_1 \int_0^{\|p_j - p_{bk}\|} \hat{B}_1 l_{jk} d l_{jk}}{v_j^T v_j}$$
$$- \frac{(\dot{v}_j - \dot{v}_i) \sum_{i=1}^{n} a_{ji} f_2 \int_0^{\|p_j - p_i\|} \hat{B}_2 m_{ji} d m_{ji}}{(v_j^T - v_i^T)(v_j - v_i)}$$

$$+\frac{(\dot{v}_j - \dot{v}_i)\sum_{i=1}^{n} a_{ji}f_3 \int_0^{\|p_j - p_i\|} \hat{B}_3 m_{ji} dm_{ji}}{(v_j^T - v_i^T)(v_j - v_i)} \quad (15)$$

where if the formation tends to be stable, the target avoidance function $\hat{B}_1 = \hat{B}_2 = \hat{B}_3 = 0$, therefore the function $r_{or}(t)$ is bounded. If the formation doesn't tend to be stable, the quadrotor have different speed with neighboring quadrotor ($v_j \neq v_i$), so the $r_{or}(t)$ is bounded and it has a bunch of upper bounds $\|r_{or}(t)\| < r_{or0}$, $\|\dot{r}_{or}(t)\| < r_{or1}$, $\|\ddot{r}_{or}(t)\| < r_{or2}$, where $r_{or0}, r_{or1}, r_{or2}$ are unknown constants.

During the sliding motion $\rho_j(t) \equiv 0$, the so-called equivalent control $U_{eq}(t)$ is designed, which must take on average to maintain sliding. To make sure $\dot{\rho}_j(t) = 0$, $\rho_j(t) = 0$, with in definition I, $U_{eq}(t)$ must satisfy

$$U_{eq}(t) = -r_{or}(t) \quad (16)$$

So, there is $\|U_{eq}(t)\| = \|r_{or}(t)\|$ during sliding. In order to obtain the estimate value of $U_{eq}(t)$, it can be performed by low-pass filter. In this way, $U_{eq}(t)$ can be got as follow:

$$\dot{\bar{U}}_{eq}(t) = \frac{1}{\kappa_1}(U_{eq}(t) - \bar{U}_{eq}(t)) \quad (17)$$

where κ_1 is a small constant, which is to make $\bar{U}_{eq}(t) \to U_{eq}(t)$

Assuming that $1 > \phi_{or1} > 0$, $\phi_{or0} > 0$, there is

$$\left|\|\bar{U}_{eq}(t)\| - \|U_{eq}(t)\|\right| < \phi_{or1}\|U_{eq}(t)\| + \phi_{or0} \quad (18)$$

$n(t)$ contains a nested adaption law shown as follows [37]:

$$\dot{n}(t) = -\delta_{or}(t)\left[\|\chi(t)\|^3 + \|\chi(t)\|^{\frac{1}{2}}\right] \quad (19)$$

$$\chi(t) = n(t) - \frac{1}{\beta_{or}}\|\bar{U}_{eq}(t)\| - \mu_{or} \quad (20)$$

$$\delta_{or}(t) = \sigma_0 + \sigma(t) \quad (21)$$

$$\dot{\sigma}(t) = \begin{cases} \gamma\left[\|\chi(t)\|^4 + \|\chi(t)\|^{\frac{3}{2}}\right] \\ \quad + \frac{\sigma_0}{\hat{\varepsilon}(t)}\left[\|\varepsilon(t)\|^4 + \|\varepsilon(t)\|^{\frac{3}{2}}\right], if \ \| \chi(t) \| > \chi_0 \\ \frac{\sigma_0}{\hat{\varepsilon}(t)}\left[\|\varepsilon(t)\|^4 + \|\varepsilon(t)\|^{\frac{3}{2}}\right], \\ otherwise \end{cases}$$

$$(22)$$

$$\varepsilon(t) = \frac{q_{or}r_{or2}}{\beta_{or}} - \sigma(t) \quad (23)$$

where $\hat{\varepsilon}(t) = \begin{cases} \varepsilon(t) & \varepsilon(t) \neq 0 \\ \varepsilon(t) + \varepsilon_0 & \varepsilon(t) = 0 \end{cases}$, $\varepsilon_0 > 0$ is a small constant, $\gamma > 0, \sigma_0 > 0, 0 < \beta_{or} < 1$ and $\mu_{or} > 0$ are design scalars to make sure

$$\frac{1}{\beta_{or}}\|\bar{U}_{eq}(t)\| + \frac{\mu_{or}}{2} > \|U_{eq}(t)\| \quad (24)$$

In order to limit the low bound of $n(t)$, there is

$$n(t) > \frac{1}{\beta_{or}}\|\bar{U}_{eq}(t)\| + \mu_{or} \quad (25)$$

Theorem 1: For system (1), the sliding surface ρ_j converges to set $D_\rho = \left\{\rho_j | \|\rho_j\| \leq \upsilon_\rho \triangleq \max(\upsilon_0, \upsilon_{V_1})\right\}$ with

$0 < \mu_a < 1$ in a uniformly bounded settling time $T_{11} \leq T_{11}^* \triangleq \frac{d_1(\gamma(\frac{4}{\mu_a c_1(1-\gamma_1)} + \frac{1}{\mu_a c_2(\alpha_1-1)}))}{\iota_1} + \frac{4}{\mu_a c_1(1-\gamma_1)} + \frac{1}{\mu_a c_2(\alpha_1-1)}$, where $\gamma_1 = \frac{3}{4}, \alpha_1 = 2$ when the controller shown as

$$U_{oj} = \begin{cases} U_j & X \in \mathbb{R}^2 \backslash \hat{\Omega} \\ U_j^* & X \in \hat{\Omega} \end{cases} \quad (26)$$

where $\mathbb{R}^2$ is the error domain, $\hat{\Omega}$ is the singular region

$$U_j = -m_j(\beta_1 + \sum_{k=1}^{n} f_1\hat{B}_1(\|p_j - p_{bk}\|)(p_j - p_{bk})$$

$$-\sum_{i=1}^{n} a_{ji}f_2\hat{B}_2(\|p_j - p_i\|)(p_j - p_i)$$

$$+\sum_{i=1}^{n} a_{ji}f_3\hat{B}_3(\|p_j - p_i\|)(p_j - p_i)$$

$$-n(t)sign(\rho_j) - ((\frac{1}{2})^2\Lambda_1\|\rho_j\|^2\rho_j$$

$$+(\frac{1}{2})^{\frac{3}{4}}\Lambda_2\frac{\Theta}{\|\rho_j\|^2}\rho_j))$$

$$+\iota_1\left[\hat{S}(d_1'(y))\right]^{-2}\hat{S}(d_1''(y))\dot{y}/\sum_{i=0}^{n} a_{ji} \quad (27)$$

$$U_j^* = -m_j(\beta_1 + \sum_{k=1}^{n} f_1\hat{B}_1(\|p_j - p_{bk}\|)(p_j - p_{bk})$$

$$-\sum_{i=1}^{n} a_{ji}f_2\hat{B}_2(\|p_j - p_i\|)(p_j - p_i)$$

$$+\sum_{i=1}^{n} a_{ji}f_3\hat{B}_3(\|p_j - p_i\|)(p_j - p_i)$$

$$-sign(\dot{y})(-n(t)sign(\rho_j))$$

$$-((\frac{1}{2})^2\Lambda_1\|\rho_j\|^2\rho_j$$

$$+(\frac{1}{2})^{\frac{3}{4}}\Lambda_2\frac{\Theta}{\|\rho_j\|^2}\rho_j)))/\sum_{i=0}^{n} a_{ji} \quad (28)$$

where $f_1, f_2, f_3, \Lambda_1, \Lambda_2$ are constants and satisfy $f_1 > 0, f_2 > 0, f_3 > 0, \Lambda_1 > 0, \Lambda_2 > 0$. $sign(\dot{y}) : \mathbb{R}^3 \to \mathbb{R}^3$ denotes the matrix with element being the sign of the corresponding element of $\dot{y}$. Θ satisfies

$$\Theta = \begin{cases} \|\rho_j\|^2, \\ \quad if \ \|\rho_j\| \geq \upsilon_0 \\ \frac{5}{4}\upsilon_0^{-0.5}\|\rho_j\|^2 - \frac{1}{4}\upsilon_0^{-2.5}\|\rho_j\|^4, \\ otherwise \end{cases} \quad (29)$$

Proof: Choose the following Lyapunov function candidate

$$V_1 = \frac{1}{2}\rho_j^T\rho_j + \frac{1}{2}\chi(t)^2 + \frac{1}{2\gamma}\varepsilon(t)^2 \quad (30)$$

If $n(t) > \| r_{or}(t) \|$, it satisfies

$$\rho_j^T \dot{\rho}_j = \rho_j^T \left[r_{or}(t) + \sum_{i=0}^{n} a_{ji} \frac{U_j}{m} \right.$$

$$- \sum_{k=1}^{n} f_1 \hat{B}_1(\| p_j - p_{bk} \|)(p_j - p_{bk})$$

$$+ \sum_{i=1}^{n} a_{ji} f_2 \hat{B}_2(\| p_j - p_i \|)(p_j - p_i)$$

$$- \sum_{i=1}^{n} a_{ji} f_3 \hat{B}_3(\| p_j - p_i \|)(p_j - p_i)$$

$$\left. + \iota_1 \left[\hat{S}(d_1'(y)) \right]^{-2} \hat{S}(d_1''(y)) \dot{y} \right]$$

$$\leq -\rho_j^T \left[(\frac{1}{2})^2 \Lambda_1 \| \rho_j \|^2 \rho_j + (\frac{1}{2})^{\frac{3}{4}} \Lambda_2 \frac{\Theta}{\| \rho_j \|^2} \rho_j \right]$$

$$= -\Lambda_1 (\frac{1}{2} \rho_j^T \rho_j)^2 - \Lambda_2 (\frac{1}{2})^{\frac{3}{4}} \Theta \quad (31)$$

When $\| \rho_j \| \geq \upsilon_0$, there is $-\Lambda_2(\frac{1}{2})^{\frac{3}{4}} \Theta = -\Lambda_2(\frac{1}{2}\rho_j^T\rho_j)^{\frac{3}{4}}$; When $\| \rho_j \| < \upsilon_0$, there is $-\Lambda_2(\frac{1}{2})^{\frac{3}{4}} \Theta \leq -\Lambda_2(\frac{1}{2}\rho_j^T\rho_j)^{\frac{3}{4}} + \Psi$, where $\Psi = (\frac{5^{\frac{4}{11}}}{2})^{\frac{11}{4}} \Lambda_2 \upsilon_0^{\frac{3}{2}}$. So there is always $-\Lambda_2(\frac{1}{2})^{\frac{3}{4}} \Theta \leq -\Lambda_2(\frac{1}{2}\rho_j^T\rho_j)^{\frac{3}{4}} + \Psi$.

It can be concluded as

$$\rho_j^T \dot{\rho}_j \leq -\Lambda_1 (\frac{1}{2} \rho_j^T \rho_j)^2 - \Lambda_2 (\frac{1}{2} \rho_j^T \rho_j)^{\frac{3}{4}} + \Psi \quad (32)$$

According to the (23), $\sigma > 0$ all the time, so there is $\varepsilon(t) < \frac{q_{or} r_{or2}}{\beta_{or}}$.

Note if $\chi(t) = 0$ then $n(t) = \frac{1}{\beta_{or}} \| U_{eq}(t) \| + \mu_{or} > \| U_{eq}(t) \| = \| r_{or}(t) \|$

$$\dot{\chi}(t) = \dot{n}(t) - \frac{1}{\beta_{or}} \| \dot{U}_{eq}(t) \|$$

$$= -(\sigma_0 + \sigma(t)) \left[\| \chi(t) \|^3 + \| \chi(t) \|^{\frac{1}{2}} \right]$$

$$- \frac{1}{\beta_{or}} \| \dot{U}_{eq}(t) \|$$

$$= -(\sigma_0 + \frac{q_{or} r_{or2}}{\beta_{or}} - \varepsilon(t))$$

$$\left[\| \chi(t) \|^3 + \| \chi(t) \|^{\frac{1}{2}} \right] - \frac{1}{\beta_{or}} \| \dot{U}_{eq}(t) \| \quad (33)$$

$$\chi(t)\dot{\chi}(t) = -(\sigma_0 + \sigma(t)) \left[\| \chi(t) \|^4 + \| \chi(t) \|^{\frac{3}{2}} \right]$$

$$- \frac{\| \chi(t) \|}{\beta_{or}} \| \dot{U}_{eq}(t) \|$$

$$\leq -(\sigma_0 + \frac{q_{or} r_{or2}}{\beta_{or}} - \sigma(t))$$

$$\left[\| \chi(t) \|^4 + \| \chi(t) \|^{\frac{3}{2}} \right] + \frac{\| \chi(t) \|}{\beta_{or}} \| \dot{U}_{eq}(t) \|$$

$$\leq -(\sigma_0 + \frac{q_{or} r_{or2}}{\beta_{or}} - \varepsilon(t))$$

$$\left[\| \chi(t) \|^4 + \| \chi(t) \|^{\frac{3}{2}} \right]$$

$$+ \frac{\left[\| \chi(t) \|^4 + \| \chi(t) \|^{\frac{3}{2}} \right]}{\beta_{or}} \| \dot{U}_{eq}(t) \|$$

$$\leq -\sigma_0 \left[\| \chi(t) \|^4 + \| \chi(t) \|^{\frac{3}{2}} \right]$$

$$- \frac{q_{or} r_{or2}}{\beta_{or}} \left[\| \chi(t) \|^4 + \| \chi(t) \|^{\frac{3}{2}} \right]$$

$$+ \varepsilon(t) \left[\| \chi(t) \|^4 + \| \chi(t) \|^{\frac{3}{2}} \right]$$

$$+ \frac{q_{or} r_{or2}}{\beta_{or}} \left[\| \chi(t) \|^4 + \| \chi(t) \|^{\frac{3}{2}} \right]$$

$$= -\sigma_0 \left[\| \chi(t) \|^4 + \| \chi(t) \|^{\frac{3}{2}} \right]$$

$$+ \varepsilon(t) \left[\| \chi(t) \|^4 + \| \chi(t) \|^{\frac{3}{2}} \right] \quad (34)$$

To prove the stability of outer-loop, consider two conditions in the following proof.

Case a). $\| \chi(t) \| > \chi_0$

According to $\varepsilon(t)$ in (23), the first-order derivative of can be described as:

$$\dot{\varepsilon}(t) = -\sigma(t)$$

$$= -\gamma \left[\| \chi(t) \|^4 + \| \chi(t) \|^{\frac{3}{2}} \right]$$

$$- \frac{\sigma_0}{\varepsilon(t)} \left[\| \varepsilon(t) \|^4 + \| \varepsilon(t) \|^{\frac{3}{2}} \right] \quad (35)$$

Substitute (32), (34) and (35) to (30), there is

$$\dot{V}_1 \leq -\Lambda_1 (\frac{1}{2} \rho_j^T \rho_j)^2 - \Lambda_2 (\frac{1}{2} \rho_j^T \rho_j)^{\frac{3}{4}} + \Psi$$

$$- \sigma_0 \left[\| \chi(t) \|^4 + \| \chi(t) \|^{\frac{3}{2}} \right]$$

$$+ \varepsilon(t) \left[\| \chi(t) \|^4 + \| \chi(t) \|^{\frac{3}{2}} \right]$$

$$- \varepsilon(t) \left[\| \chi(t) \|^4 + \| \chi(t) \|^{\frac{3}{2}} \right]$$

$$- \frac{\sigma_0}{\gamma} \left[\| \varepsilon(t) \|^4 + \| \varepsilon(t) \|^{\frac{3}{2}} \right]$$

$$= -\Lambda_1 (\frac{1}{2} \rho_j^T \rho_j)^2 - \Lambda_2 (\frac{1}{2} \rho_j^T \rho_j)^{\frac{3}{4}} + \Psi$$

$$- \sigma_0 \left[\| \chi(t) \|^4 + \| \chi(t) \|^{\frac{3}{2}} \right]$$

$$- \frac{\sigma_0}{\gamma} \left[\| \varepsilon(t) \|^4 + \| \varepsilon(t) \|^{\frac{3}{2}} \right]$$

$$\leq -c_1 V_1^2 - c_2 V_1^{\frac{3}{4}} + \Psi \quad (36)$$

where $c_1 = \min(\Lambda_1, \sigma_0, \frac{\sigma_0}{\gamma})$, $c_2 = \min(\Lambda_2, \sigma_0, \frac{\sigma_0}{\gamma})$

Case b). $\| \chi(t) \| \leq \chi_0$

From (22), there is $\dot{\sigma}(t) = 0$ and based on the definition of $\varepsilon(t)$ given by (23), it follows that

$$\dot{\varepsilon}(t) = -\sigma(t) = -\frac{\sigma_0}{\varepsilon(t)} \left[\| \varepsilon(t) \|^4 + \| \varepsilon(t) \|^{\frac{3}{2}} \right] \quad (37)$$

Substitute (32), (34) and (37) to (30), it follows that

$$\dot{V}_1 \leq -\Lambda_1 (\frac{1}{2} \rho_j^T \rho_j)^2 - \Lambda_2 (\frac{1}{2} \rho_j^T \rho_j)^{\frac{3}{4}} + \Psi$$

$$- \sigma_0 \left[\| \chi(t) \|^4 + \| \chi(t) \|^{\frac{3}{2}} \right]$$

$$+ \varepsilon(t) \left[\| \chi(t) \|^4 + \| \chi(t) \|^{\frac{3}{2}} \right]$$

$$-\frac{\sigma_0}{\gamma}\left[\|\varepsilon(t)\|^4 + \|\varepsilon(t)\|^{\frac{3}{2}}\right] \tag{38}$$

Consequently, outside of following rectangular region, which is the solution domain

$$\Xi = \left\{(\chi, \varepsilon) : \|\chi\| < \chi_0, 0 \le \varepsilon < \frac{q_{or}r_{or2}}{\beta_{or}}\right\} \tag{39}$$

the condition

$$\dot{V}_1 \le -\Lambda_1 (\tfrac{1}{2}\rho_j^T \rho_j)^2 - \Lambda_2 (\tfrac{1}{2}\rho_j^T \rho_j)^{\frac{3}{4}} + \Psi$$
$$-\sigma_0 \left[\|\chi(t)\|^4 + \|\chi(t)\|^{\frac{3}{2}}\right]$$
$$-\frac{\sigma_0}{\gamma}\left[\|\varepsilon(t)\|^4 + \|\varepsilon(t)\|^{\frac{3}{2}}\right] \tag{40}$$

is satisfied. So, we construct an ellipse as follows:

$$\Phi = \{(\chi, \varepsilon) : V(\chi, \varepsilon) < \psi\} \tag{41}$$
$$\psi = \frac{1}{2}\chi_0^2 + \frac{1}{\gamma}(\frac{q_{or}r_{or2}}{\beta_{or}})^2 \tag{42}$$

where $\chi(t)$ is the X-axis, $\varepsilon(t)$ is the Y-axis. The ellipse contains a rectangular, whose width is ξ_0, and the height is $\frac{q_{or}r_{or2}}{\beta_{or}}$.

Then the error $\chi(t)$ in (20) will satisfy $\chi(t) < \frac{\mu_{or}}{2}$ in fixed time and there is

$$\|\chi(t)\| = \left\|n(t) - \frac{1}{\beta_{or}}\|\bar{U}_{eq}(t)\| - \mu_{or}\right\| < \frac{1}{2}\mu_{or} \tag{43}$$

So, according to the (24) and (25), the following inequality can be concluded:

$$n(t) > \frac{1}{\beta_{or}}\|\bar{U}_{eq}(t)\| + \frac{\mu_{or}}{2}$$
$$> \|U_{eq}(t)\| = \|r_{or}(t)\| \tag{44}$$

The remaining proof follows the procedure in [37], and the inequality can be concluded

$$\dot{V}_1 \le -c_1 V_1^2 - c_2 V_1^{\frac{3}{4}} + \Psi \tag{45}$$

Thus the sliding surface ρ_j can converge to zero in fixed time.

Nevertheless, once the sliding surface converges to zero, in other words, the actual position of the quadrotor is close to the desired trajectory, with (8) and (11), there is $\dot{y} = -\iota_1\left[\hat{S}(d_1'(y))\right]^{-1}E_1$. As mentioned in the definition I, $\lim_{y\to 0}\left[\hat{S}(d_1'(y))\right]^{-1} = 0$, if at this point $\dot{y} \ne 0$, it will give rise to the singularity problem. The solution is given below.

Set the plane coordinate system with y as the X-axis and $\dot{y}$ as the Y-axis, design a small neighborhood region when the sliding mode $y = 0$, the width is ε, that is $\Omega \triangleq \{X \in R^2| - \varepsilon < y < \varepsilon\}$, in which $X = [y, \dot{y}]^T$, and the control input will be modified in the region. Let the trajectory directly across this region, so that it can avoid the singularity. In $\dot{y} > 0, y < 0$ and $\dot{y} < 0, y > 0$ these two regions, which are the critical areas, design four regions B_1, B_2, B_3, B_4, which denote the four quadrants of the plane,

and $B_1 \triangleq \{X|y > 0, \dot{y} > 0\}$, $B_2 \triangleq \{X|y < 0, \dot{y} > 0\}$, $B_3 \triangleq \{X|y < 0, \dot{y} < 0\}$, $B_4 \triangleq \{X|y > 0, \dot{y} < 0\}$. According to what was mentioned above, to prove that it converges at a fixed time, $y\dot{y} > 0$ is needed, and it is clearly observed in B_1 and B_3. Thus, the control input doesn't need to change in these fields. Otherwise, the trajectory of the system must intercept the sliding surface before $y = 0$ in the fields. So, the singularity can be compensated by sliding mode.

To a certain extent, the field Ω can narrowed down by choosing ι_1. Corresponding to any $X^* \in B_2$ or $X^* \in B_4$, there will always be one big enough $\iota_1 > 0$, making $X^* \in B_2 \backslash A^+$, $X^* \in B_4 \backslash A^-$. At the same time, the bigger ι_1 is, the faster the sliding mode stability time is, that is, the better the convergence is. Set boundaries for variables $j(t) - |d_U| \ge k$, and $k > 0$. Moreover, it can always be $\bar{j}(t) = j(t) + k$ by design, where $j(t)$ is an adaptive variable to eliminate the error defined as $j(t) = -n(t)sign(\rho_j) - ((\frac{1}{2})^2\Lambda_1\|\rho_j\|^2\rho_j + (\frac{1}{2})^{\frac{3}{4}}\Lambda_2\frac{\Theta}{\|\rho_j\|^2}\rho_j))$.

Considering that the solution to the differential equation might be in reverse time region $t \in (-\infty, 0]$, define the curve $\Psi^{\pm} = \{X|X = \varphi^{\pm}\}$. By constructing, there is no singularity in a closed region of $\Psi^{\pm}, \varphi^{\pm}, \rho_j^{\pm}$. In this inverse time system, the worst-case scenario is $j(t) - |d_U| \equiv k$, but according to the outer-loop system (1), there is $d_{Uj} = m_j\dot{v}_j - m_jge_3 + T_jR(Q_j)^Te_3$, $\dot{v}_j$ is a variable over time. So, $j(t) - |d_U| \equiv k$ is impossible to be satisfied forever. In the general case, the discontinuous U_j of the input is guaranteed to converge to the sliding surface. Therefore, when the initial value is within $s^{\pm}$, $y^*, \dot{y}^*$ can be guaranteed to reach the sliding mode surface under the condition of $y^* \ne 0$. Avoid singularity methods modified in $X \in \Omega\backslash(\rho_j^+ \cup \rho_j^-)$. So, by setting up the control input U^* to ensure $\ddot{y}\ddot{y} \ge 0$, at the same time there is $|\dot{y}| \ge \|\dot{y}(0)\| \ge \frac{2\iota_1}{|d_1'(y(0))|}$.

Through the above, the trajectory is going to pass through region Ω in fixed time T_Ω, and satisfy $T_\Omega \le \max \iota_1\tau f_1'(\tau)$, where $\tau \in [0, \varepsilon]$. The extra time T_Ω can be seen as the cost of avoiding the singularity.

The proof is completed.

Theorem 2: As the system reaches on the sliding-mode surface $\rho_j(t) = 0$, the error of the position will converge to zero and the system tends to be stable in fixed time.

Proof: When the system is on the sliding-mode $\rho_j(t) = 0$, the safety function $A^o = 0$, and there is

$$e_{vj} = -k_1 e_{pj}\|e_{pj}\| - k_2 e_{pj}\|e_{pj}\|^{-\frac{1}{2}} \tag{46}$$

Choose the following lyapunov function

$$V_3 = \frac{1}{2}e_{pj}^T e_{pj} \tag{47}$$

the time derivative of V_3 is calculated as

$$\dot{V}_3 = e_{pj}^T \dot{e}_{pj}$$
$$= e_{pj}^T\left(-k_1 e_{pj}\|e_{pj}\| - k_2 e_{pj}\|e_{pj}\|^{-\frac{1}{2}}\right)$$

$$= -k_1 \left\| e_{pj} \right\|^3 - k_2 \left\| e_{pj} \right\|^{\frac{3}{2}}$$

$$= -K_1 V_3^{\frac{3}{2}} - K_2 V_3^{\frac{3}{4}} \tag{48}$$

where K_1 and K_2 are two positive constants and are given as $K_1 = \frac{k_1}{2^{\frac{3}{2}}}, K_2 = \frac{k_2}{2^{\frac{3}{4}}}$

The fixed settling time T_{12} is bounded by

$$T_{12} \leq \frac{2}{K_1} + \frac{4}{K_2} \tag{49}$$

Thus, the outer-loop convergence time T_1 is bounded by

$$T_1 \leq T_{11} + T_{12} \tag{50}$$

The whole outer-loop proof is completed.

Remark 3: In order to ensure the good performance of the system, f_1, f_2, f_3 are chosen as $f_1 > 0, f_2 > 0, f_3 > 0$. The defined parameters μ_{or} and β_{or} are the safety factors. χ_0 is larger than noise error, and it is selected as a small positive constant. q_{or} reflects the accuracy associated with the estimated equivalent control. The impact of the parameter σ_0 on the system is slight, and it is suggested to be set in the range of $\sigma_0 > 0$.

B. THE INNER-LOOP SYSTEM STABILITY ANALYSIS

Define the angular velocity error $\tilde{\omega}_j = \omega_j - R(\tilde{Q}_j)\omega_{dj}$, where ω_{dj} is the desired angular velocity and defined as

$$\omega_{dj} = 2 \begin{bmatrix} \eta_{dj} I_3 + S(q_{dj}) \\ -q_{dj}^T \end{bmatrix}^T \dot{Q}_{dj} \tag{51}$$

Consider the first-order sliding mode equation as follow:

$$x_j(t) = k_3 \tilde{q}_j \left\| \tilde{q}_j \right\| + k_4 \tilde{q}_j \left\| \tilde{q}_j \right\|^{-\frac{1}{2}} + \tilde{\omega}_j$$
$$+ \iota_2 \left[\hat{S}(d_1{}'(a)) \right]^{-1} E_1 \tag{52}$$

Similarly to the outer-loop, a is a dynamic variable and defined as

$$\dot{a} = k_3 \tilde{q}_j \left\| \tilde{q}_j \right\| + k_4 \tilde{q}_j \left\| \tilde{q}_j \right\|^{-\frac{1}{2}} + \tilde{\omega}_j \tag{53}$$

Take the time derivative of $x_j(t)$ yields

$$\dot{x}_j(t) = \beta_2 + \dot{\omega}_j + S(\tilde{\omega}_j)R(\tilde{Q}_j)\omega_{dj} - R(\tilde{Q}_j)\dot{\omega}_{dj}$$
$$+ \iota_2 \left[\hat{S}(d_1{}'(a)) \right]^{-2} \hat{S}\left(d_1{}''(a) \right) \dot{a}$$
$$= \beta_2 - I_{fj}^{-1} S(\omega_j)I_{fj}\omega_j + I_{fj}^{-1} d_{\Gamma_j}$$
$$+ S(\tilde{\omega}_j)R(\tilde{Q}_J)\omega_{dj} - R(\tilde{Q}_j)\tilde{\omega}_{dj}$$
$$+ \iota_2 \left[\hat{S}(d_1{}'(a)) \right]^{-2} \hat{S}\left(d_1{}''(a) \right) \dot{a} \tag{54}$$

where

$$\beta_2 = \left[\frac{k_3}{2} \left(I + \frac{\tilde{q}_j \tilde{q}_j^T}{\left\| \tilde{q}_j \right\|^2} \right) \left\| \tilde{q}_j \right\| \right.$$
$$\left. + \frac{k_4}{2} \left(I + \frac{\tilde{q}_j \tilde{q}_j^T}{\left\| \tilde{q}_j \right\|^2} \right) \left\| \tilde{q}_j \right\|^{-\frac{1}{2}} \right] (\tilde{\eta}_j I_3 + S(\tilde{q}_j)) \tilde{\omega}_j$$

To find out the special case in the sliding process, let

$$\dot{x}_j(t) = r_{ir}(t) + \beta_2 + \Gamma(t)$$
$$+ \iota_2 \left[\hat{S}(d_1{}'(a)) \right]^{-2} \hat{S}\left(d_1{}''(a) \right) \dot{a} \tag{55}$$

where

$$r_{ir}(t) = -I_{fj}^{-1} S(\omega_j)I_{fj}\omega_j + I_{fj}^{-1} d_{\Gamma_j}$$
$$+ S(\tilde{\omega}_j)R(\tilde{Q}_j)\omega_{dj} - R(\tilde{Q}_j)\dot{\omega}_{dj} \tag{56}$$

where $\lambda_2 > 0$, I_{fj}, ω_{dj}, $\dot{\omega}_{dj}$ are bounded, so $r_{ir}(t)$ is bounded and it has a bunch of upper bounds $\|r_{ir}(t)\| < r_{ir0}$, $\|\dot{r}_{ir}(t)\| < r_{ir1}$, $\|\ddot{r}_{ir}(t)\| < r_{ir2}$, where r_{ir0}, r_{ir1}, r_{ir2} are unknown constants.

$$\Upsilon = \begin{cases} \left\| x_j(t) \right\|^2, \\ \quad \text{if } \left\| x_j(t) \right\| \geq \upsilon_1 \\ \frac{5}{4} \upsilon_1^{-0.5} \left\| x_j(t) \right\|^2 - \frac{1}{4} \upsilon_1^{-2.5} \left\| x_j(t) \right\|^4, \\ \quad \text{otherwise} \end{cases} \tag{57}$$

During the sliding motion $x_j(t) \equiv 0$, design the so-called equivalent control $\Gamma_{eq}(t)$, which must take on average to maintain sliding. To make sure that $\dot{x}_j(t) = 0$, $x_j(t) = 0$, with $d_1{}'(a) = 0$ in definition, $\Gamma_{eq}(t)$ must satisfy $\Gamma_{eq}(t) = -r_{ir}(t)$. So, there is $\left\| \Gamma_{eq}(t) \right\| = \|r_{ir}(t)\|$ during sliding. In order to obtain the estimate value of $\Gamma_{eq}(t)$, it can be performed by low-pass filtering. In this way, $\Gamma_{eq}(t)$ is got as follows:

$$\dot{\bar{\Gamma}}_{eq}(t) = \frac{1}{\kappa_2}(\Gamma_{eq}(t) - \bar{\Gamma}_{eq}(t)) \tag{58}$$

where κ_2 is a small constant, which is to make $\bar{\Gamma}_{eq}(t) \to \Gamma_{eq}(t)$

Assuming that $1 > \phi_{ir1} > 0$, $\phi_{ir0} > 0$, there is

$$\left| \left\| \bar{\Gamma}_{eq}(t) \right\| - \left\| \Gamma_{eq}(t) \right\| \right| < \phi_{ir1} \left\| \Gamma_{eq}(t) \right\| + \phi_{ir0} \tag{59}$$

$s(t)$ contains a nested adaption law shown as follows:

$$\dot{s}(t) = -\delta_{ir}(t) \left[\|\xi(t)\|^3 + \|\xi(t)\|^{\frac{1}{2}} \right] \tag{60}$$

$$\xi(t) = s(t) - \frac{1}{\beta_{ir}} \left\| \bar{\Gamma}_{eq}(t) \right\| - \mu_{ir} \tag{61}$$

$$\delta_{ir}(t) = b_0 + b(t) \tag{62}$$

$$\dot{b}(t) = \begin{cases} \varpi \left[\|\xi(t)\|^4 + \|\xi(t)\|^{\frac{3}{2}} \right] \\ + \frac{b_0}{\hat{\varsigma}(t)} \left[\|\varsigma(t)\|^4 + \|\varsigma(t)\|^{\frac{3}{2}} \right], \text{ if } \| \xi(t) \| > \xi_0 \\ \frac{b_0}{\hat{\varsigma}(t)} \left[\|\varsigma(t)\|^4 + \|\varsigma(t)\|^{\frac{3}{2}} \right], \\ \quad \text{otherwise} \end{cases} \tag{63}$$

$$\varsigma(t) = \frac{q_{ir} r_{ir2}}{\beta_{ir}} - b(t) \tag{64}$$

where $\hat{\varsigma}(t) = \begin{cases} \varsigma(t) & \varsigma(t) \neq 0 \\ \varsigma(t) + \varsigma_0 & \varsigma(t) = 0 \end{cases}$, $\varsigma_0 > 0$ is a small constant, $\varpi > 0$, $b_0 > 0$, $0 < \beta_{ir} < 1$ and $\mu_{ir} > 0$ are design scalars to make sure

$$\frac{1}{\beta_{ir}} \left\| \bar{\Gamma}_{eq}(t) \right\| + \frac{\mu_{ir}}{2} > \left\| \Gamma_{eq}(t) \right\| \tag{65}$$

A lower-bound of $s(t)$ is provided, and the goal is to ensure

$$s(t) > \frac{1}{\beta_{ir}} \|\bar{\Gamma}_{eq}(t)\| + \mu_{ir} \quad (66)$$

Theorem 3: For the system (2), with the fixed time $T_{21} \leq T_{21}^* \triangleq \frac{d_1(a(\frac{4}{\mu_b c_2(1-\gamma_2)} + \frac{1}{\mu_b c_4(\alpha_2-1)}))}{\iota_2} + \frac{4}{\mu_a c_1(1-\gamma_1)} + \frac{1}{\mu_a c_2(\alpha_1-1)}$, the sliding surface x_j converges to set $D_x = \{x_j | \|x_j\| \leq \upsilon_x \triangleq \max(\upsilon_1, \upsilon_{V_2})\}$, where $0 < \mu_b < 1$, $\gamma_2 = \frac{3}{4}$, $\alpha_2 = 2$, and the fixed-time robust stability of the system is proved.

The virtual attitude control Γ_j is designed as follows:

$$\Gamma_{oj} = \begin{cases} \Gamma_j & X \in \mathbb{R}^2 \setminus \breve{\Omega} \\ \Gamma_j^* & X \in \breve{\Omega} \end{cases} \quad (67)$$

where $\mathbb{R}^2$ is the error domain, $\breve{\Omega}$ is the singular region

$$\Gamma_j = \beta_2 - I_{fj}(s(t)sign(x_j) + (\frac{1}{2})^2 \Lambda_3 \|x_j(t)\|^2 x_j(t)$$
$$+ (\frac{1}{2})^{\frac{3}{4}} \Lambda_4 \frac{\Upsilon}{\|x_j(t)\|^2} x_j(t)$$
$$+ \iota_2 [\hat{S}(d_1'(a))]^{-2} \hat{S}(d_1''(a)) \dot{a} \quad (68)$$
$$\Gamma_j^* = \beta_2 - sign(\dot{a}) I_{fj}(s(t)sign(x_j)$$
$$+ (\frac{1}{2})^2 \Lambda_3 \|x_j(t)\|^2 x_j(t) + (\frac{1}{2})^{\frac{3}{4}} \Lambda_4 \frac{\Upsilon}{\|x_j(t)\|^2} x_j(t) \quad (69)$$

where Λ_3, Λ_4 are constants and satisfy $\Lambda_3 > 0$, $\Lambda_4 > 0$.

Proof: Choose the following Lyapunov function candidate

$$V_2 = \frac{1}{2} x_j^T x_j + \frac{1}{2} \xi(t)^2 + \frac{1}{2\varpi} \varsigma(t)^2 \quad (70)$$

If $s(t) > \|r_{ir}(t)\|$, it satisfies

$$x_j^T \dot{x}_j = x_j^T \left(r_{ir}(t) + u(t) + \iota_2 [\hat{S}(d_2'(a))]^{-2} \hat{S}(d_1''(a)) \dot{a} \right)$$
$$\leq -x_j^T \left((\frac{1}{2})^2 \Lambda_3 \|x_j\|^2 x_j + (\frac{1}{2})^{\frac{3}{4}} \Lambda_4 \frac{\Upsilon}{\|x_j\|^2} x_j \right)$$
$$= -\Lambda_3 \left(\frac{1}{2} x_j^T x_j \right)^2 - \Lambda_4 (\frac{1}{2})^{\frac{3}{4}} \Upsilon \quad (71)$$

when $\|x_j\| \geq \upsilon_1$, there is

$$-\Lambda_4 (\frac{1}{2})^{\frac{3}{4}} \Upsilon = -\Lambda_4 (\frac{1}{2} x_j^T x_j)^{\frac{3}{4}} \quad (72)$$

when $\|x_j\| < \upsilon_1$, there is

$$-\Lambda_4 (\frac{1}{2})^{\frac{3}{4}} \Upsilon \leq -\Lambda_4 (\frac{1}{2} x_j^T x_j)^{\frac{3}{4}} + \hat{\Psi} \quad (73)$$

where $\hat{\Psi} = (\frac{5^{\frac{4}{11}}}{2})^{\frac{11}{4}} \Lambda_4 \upsilon_1^{\frac{3}{2}}$ so $-\Lambda_4 (\frac{1}{2})^{\frac{3}{4}} \Upsilon \leq -\Lambda_4 (\frac{1}{2} x^T x)^{\frac{3}{4}} + \hat{\Psi}$.
So there is

$$x_j^T \dot{x}_j \leq -\Lambda_3 \left(\frac{1}{2} x_j^T x_j \right)^2 - \Lambda_4 (\frac{1}{2} x_j^T x_j)^{\frac{3}{4}} + \hat{\Psi} \quad (74)$$

Note if $\xi(t) = 0$ then $s(t) = \frac{1}{\beta_{ir}} \|\bar{\Gamma}_{eq}(t)\| + \mu_{ir} > \|\Gamma_{eq}(t)\| = \|r_{ir}(t)\|$

$$\dot{\xi}(t)$$
$$= \dot{s}(t) - \frac{1}{\beta_{ir}} \|\dot{\bar{\Gamma}}_{eq}(t)\|$$
$$= -(b_0 + b(t)) \left[\|\xi(t)\|^3 + \|\xi(t)\|^{\frac{1}{2}} \right] - \frac{1}{\beta_{ir}} \|\dot{\bar{\Gamma}}_{eq}(t)\|$$
$$= -(z_0 + \frac{q_{ir} r_{ir2}}{\beta_{ir}} - \varsigma(t)) \left[\|\xi(t)\|^3 + \|\xi(t)\|^{\frac{1}{2}} \right]$$
$$- \frac{1}{\beta_{ir}} \|\dot{\bar{\Gamma}}_{eq}(t)\| \quad (75)$$

$$\xi(t)\dot{\xi}(t)$$
$$= -(b_0 + b(t)) \left[\|\xi(t)\|^4 + \|\xi(t)\|^{\frac{3}{2}} \right] - \frac{\xi}{\beta_{ir}} \|\dot{\bar{\Gamma}}_{eq}(t)\|$$
$$\leq -(b_0 + \frac{q_{ir} r_{ir2}}{\beta_{ir}} - \varsigma(t)) \left[\|\xi(t)\|^4 + \|\xi(t)\|^{\frac{3}{2}} \right]$$
$$+ \frac{\left[\|\xi(t)\|^4 + \|\xi(t)\|^{\frac{3}{2}} \right]}{\beta_{ir}} \|\dot{\bar{\Gamma}}_{eq}(t)\|$$
$$\leq -b_0 \left[\|\xi(t)\|^4 + \|\xi(t)\|^{\frac{3}{2}} \right]$$
$$- \frac{q_{ir} r_{ir2}}{\beta_{ir}} \left[\|\xi(t)\|^4 + \|\xi(t)\|^{\frac{3}{2}} \right]$$
$$+ \varsigma(t) \left[\|\xi(t)\|^4 + \|\xi(t)\|^{\frac{3}{2}} \right]$$
$$+ \frac{q_{ir} r_{ir2}}{\beta_{ir}} \left[\|\xi(t)\|^4 + \|\xi(t)\|^{\frac{3}{2}} \right]$$
$$= -b_0 \left[\|\xi(t)\|^4 + \|\xi(t)\|^{\frac{3}{2}} \right] + \varsigma(t) \left[\|\xi(t)\|^4 + \|\xi(t)\|^{\frac{3}{2}} \right] \quad (76)$$

To prove the stability of inner-loop, consider two conditions in the following proof.
Case a). $\|\xi(t)\| > \xi_0$
According to $\varsigma(t)$ in (64), the first-order derivative of $\varsigma(t)$ as

$$\dot{\varsigma}(t) = -b(t)$$
$$= -\varpi \left[\|\xi(t)\|^4 + \|\xi(t)\|^{\frac{3}{2}} \right]$$
$$- \frac{b_0}{\varsigma(t)} \left[\|\varsigma(t)\|^4 + \|\varsigma(t)\|^{\frac{3}{2}} \right] \quad (77)$$

Substitute (74), (76) and (77) to (70), it follows that

$$\dot{V}_2 \leq -\Lambda_3 (\frac{1}{2} x_j^T x_j)^2 - \Lambda_4 (\frac{1}{2} x_j^T x_j)^{\frac{3}{4}} + \hat{\Psi}$$
$$- b_0 \left[\|\xi(t)\|^4 + \|\xi(t)\|^{\frac{3}{2}} \right]$$
$$+ \zeta(t) \left[\|\xi(t)\|^4 + \|\xi(t)\|^{\frac{3}{2}} \right]$$
$$- \zeta(t) \left[\|\xi(t)\|^4 + \|\xi(t)\|^{\frac{3}{2}} \right]$$
$$- \frac{b_0}{\varpi} \left[\|\xi(t)\|^4 + \|\xi(t)\|^{\frac{3}{2}} \right]$$
$$= -\Lambda_3 (\frac{1}{2} x_j^T x_j)^2 - \Lambda_4 (\frac{1}{2} x_j^T x_j)^{\frac{3}{4}} + \hat{\Psi}$$
$$- b_0 \left[\|\xi(t)\|^4 + \|\xi(t)\|^{\frac{3}{2}} \right]$$

$$-\frac{b_0}{\varpi}\left[\|\zeta(t)\|^4 + \|\zeta(t)\|^{\frac{3}{2}}\right]$$

$$\leq -c_3 V_2^2 - c_4 V_2^{\frac{3}{4}} + \hat{\Psi} \tag{78}$$

where $c_3 = \min(\Lambda_3, b_0, \frac{b_0}{\varpi})$, $c_4 = \min(\Lambda_4, b_0, \frac{b_0}{\varpi})$

Case b.) $\|\xi(t)\| \leq \xi_0$

From (63), there is $b(t) = 0$ and based on the definition of $\varsigma(t)$ given by (64), there is

$$\dot{\varsigma}(t) = -b(t) = -\frac{b_0}{\varsigma(t)}\left[\|\varsigma(t)\|^4 + \|\varsigma(t)\|^{\frac{3}{2}}\right] \tag{79}$$

Substitute (74), (76) and (79) to (70), there is

$$\dot{V}_2 \leq -\Lambda_3(\frac{1}{2}x_j^T x_j)^2 - \Lambda_4(\frac{1}{2}x_j^T x_j)^{\frac{3}{4}} + \hat{\Psi}$$

$$-b_0\left[\|\xi(t)\|^4 + \|\xi(t)\|^{\frac{3}{2}}\right]$$

$$+\varsigma(t)\left[\|\xi(t)\|^4 + \|\xi(t)\|^{\frac{3}{2}}\right]$$

$$-\frac{b_0}{\varpi}\left[\|\varsigma(t)\|^4 + \|\varsigma(t)\|^{\frac{3}{2}}\right] \tag{80}$$

Consequently, it's proved that outside the following rectangular region:

$$\tau = \left\{(\xi, \varsigma) : \|\xi\| < \xi_0, 0 \leq \varsigma < \frac{q_{ir} r_{ir2}}{\beta_{ir}}\right\} \tag{81}$$

the inequality

$$\dot{V}_2 \leq -\Lambda_3(\frac{1}{2}x_j^T x_j)^2 - \Lambda_4(\frac{1}{2}x_j^T x_j)^{\frac{3}{4}} + \hat{\Psi}$$

$$-b_0\left[\|\xi(t)\|^4 + \|\xi(t)\|^{\frac{3}{2}}\right]$$

$$-\frac{b_0}{\varpi}\left[\|\varsigma(t)\|^4 + \|\varsigma(t)\|^{\frac{3}{2}}\right] \tag{82}$$

is satisfied. So, we construct an ellipse as follows:

$$N = \{(\xi, \varsigma) : V(\xi, \varsigma) < \hat{\psi}\} \tag{83}$$

$$\hat{\psi} = \frac{1}{2}\xi_0^2 + \frac{1}{\varpi}(\frac{q_{ir} r_{ir2}}{\beta_{ir}})^2 \tag{84}$$

where $\xi(t)$ is the X-axis, $\varsigma(t)$ is the Y-axis. The ellipse contains a rectangular, which width is ξ_0, and the height is $\frac{q_{ir} r_{ir2}}{\beta_{ir}}$.

If the μ_{ir} can be chosen to satisfy

$$\frac{1}{4}\mu_{ir}^2 > \xi_0^2 + \frac{1}{\varpi}\left(\frac{q_{ir} r_{ir2}}{\beta_{ir}}\right)^2 \tag{85}$$

$\xi(t)$ will be forced to converge into the region of in fixed time.

According to the definition of $\xi(t)$ given by (61), there is

$$\|\xi(t)\| = \left\|s(t) - \frac{1}{\beta_{ir}}\|\bar{\Gamma}_{eq}(t)\| - \mu_{ir}\right\| < \frac{1}{2}\mu_{ir} \tag{86}$$

Based on the (65) and (66), there is

$$s(t) > \frac{1}{\beta_{ir}}\|\bar{\Gamma}_{eq}(t)\| + \frac{\mu_{ir}}{2} > \|\Gamma_{eq}(t)\| = \|r_{ir}(t)\| \tag{87}$$

The remaining proof follows the procedure in [37], and the inequality can be concluded

$$\dot{V}_2 \leq -c_3 V_2^2 - c_4 V_2^{\frac{3}{4}} + \hat{\Psi} \tag{88}$$

Thus the sliding surface x_j can converge to zero in fixed time.

Remark 4: As the sliding surface converges to zero, in other words, the quaternion tracking error of the quadrotors converges to zero, there is $\dot{a} = -\iota_1\left[\hat{S}(d_1'(a))\right]^{-1} E_1$. As exploited in the definition I, $\lim_{a \to 0}\left[\hat{S}(d_1'(a))\right]^{-1} = 0$, but if at this point $\dot{a} \neq 0$, it will give rise to the singularity problem.

The singularity avoidance in the attitude design could be similar design in outer-loop design, the field of $\breve{\Omega}$ can be narrowed down by choosing ι_2. By a series of singular-avoidance like the one in outer-loop design, the control input sets up as follows Γ_j^*.

Remark 5: The scalar ξ_0 is a small positive constant, and it is larger than noise error. The defined parameters μ_{ir} and β_{ir} are the safety factors. q_{ir} reflects the accuracy associated with the estimated equivalent control. Now, the proof is partially completed

Theorem 4: As the system reaches on the sliding-mode surface $x_j(t) = 0$, the error of the attitude will converge to zero and the system tends to be stable in fixed time.

Proof: When the system is on the sliding-mode $x_j(t) = 0$, there is

$$\tilde{\omega}_j = -k_3\tilde{q}_j\|\tilde{q}_j\| - k_4\tilde{q}_j\|\tilde{q}_j\|^{-\frac{1}{2}} \tag{89}$$

Choose the following lyapunov function

$$V_4 = \frac{1}{2}\tilde{q}_j^T \tilde{q}_j \tag{90}$$

it yields that

$$\dot{V}_4 = \tilde{q}_j^T \dot{\tilde{q}}_j$$

$$= \frac{1}{2}\tilde{q}_j^T (\tilde{\eta}_j I_3 + S(\tilde{q}_j))\tilde{\omega}_j$$

$$\leq -\frac{k_3}{2}\|\tilde{q}_j\|^3 - \frac{k_4}{2}\|\tilde{q}_j\|^{\frac{3}{2}}$$

$$\leq -K_3 V_4^{\frac{3}{2}} - K_4 V_3^{\frac{3}{4}} \tag{91}$$

where $K_3 = \frac{k_3}{2^{\frac{5}{2}}}$, $K_4 = \frac{k_4}{2^{\frac{7}{4}}}$

The fixed settling time T_{22} is bounded by

$$T_{22} \leq \frac{2}{K_3} + \frac{4}{K_4} \tag{92}$$

Thus, the inner-loop convergence time T_2 is bounded by

$$T_2 \leq T_{21} + T_{22} \tag{93}$$

The whole inner-loop proof is completed.

C. THE WHOLE CLOSED-LOOP STABILITY ANALYSIS

Theorem 5: For the outer-loop system (1) and inner-loop system (2), with a uniformly bounded settling time $T_b \leq \frac{4}{\mu_c c_5(1-\gamma_3)} + \frac{1}{\mu_c c_6(\alpha_3-1)}$, where $\gamma_3 = \frac{3}{4}, \alpha_3 = 2$, the fixed-time robust stability of the system is going to be proved.

Proof: Choose the following Lyapunov function
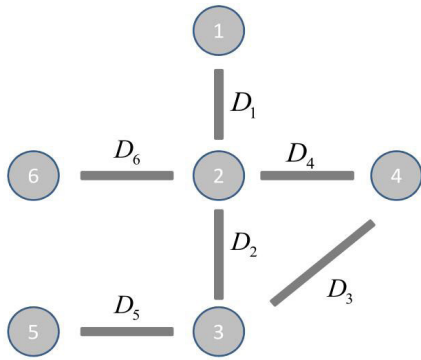
$$V_{whole} = V_1 + V_2 \tag{94}$$

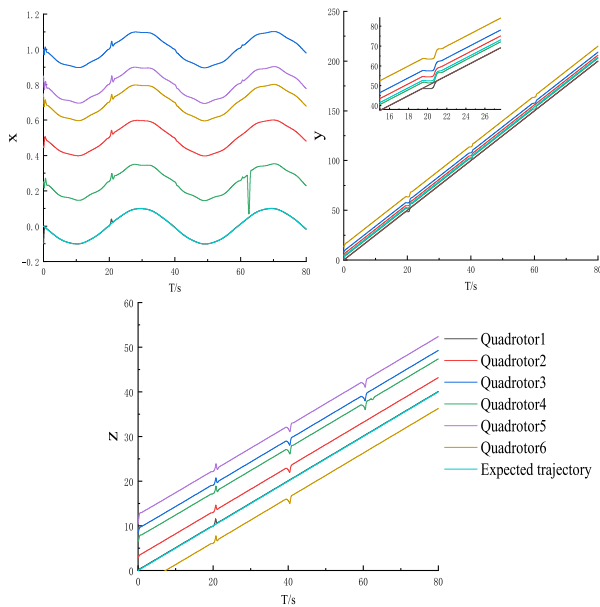**FIGURE 3.** The communication graph.

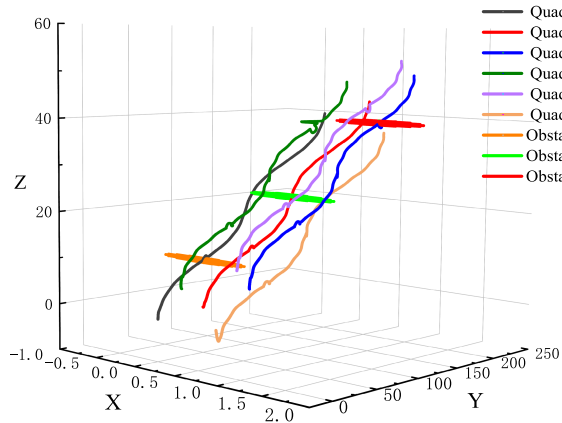**FIGURE 4.** The position of the quadrotor on the x-axis, y-axis, and z-axis.

FIGURE 5. The trajectory of six quadrotors in three dimensions.

It yields that

$$\dot{V}_{whole} = \dot{V}_1 + \dot{V}_2$$
$$= -c_1 V_1{}^2 - c_2 V_1^{\frac{3}{4}} + \Psi - c_3 V_2{}^2 - c_4 V_2^{\frac{3}{4}} + \theta$$
$$\leq -c_5 V_1{}^2 - c_6 V_1^{\frac{3}{4}} + \hat{\Theta} \qquad (95)$$

where $c_5 = \min\{c_1, c_3\}$, $c_6 = \min\{c_2, c_4\}$, $\hat{\Theta} = \Psi + \theta$
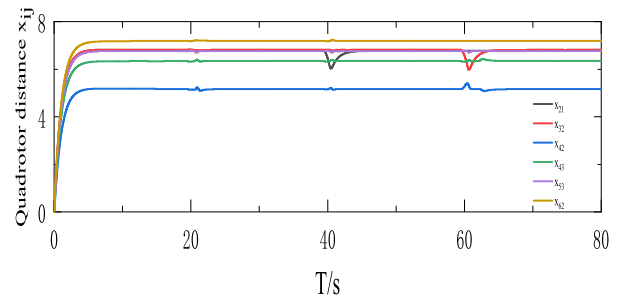
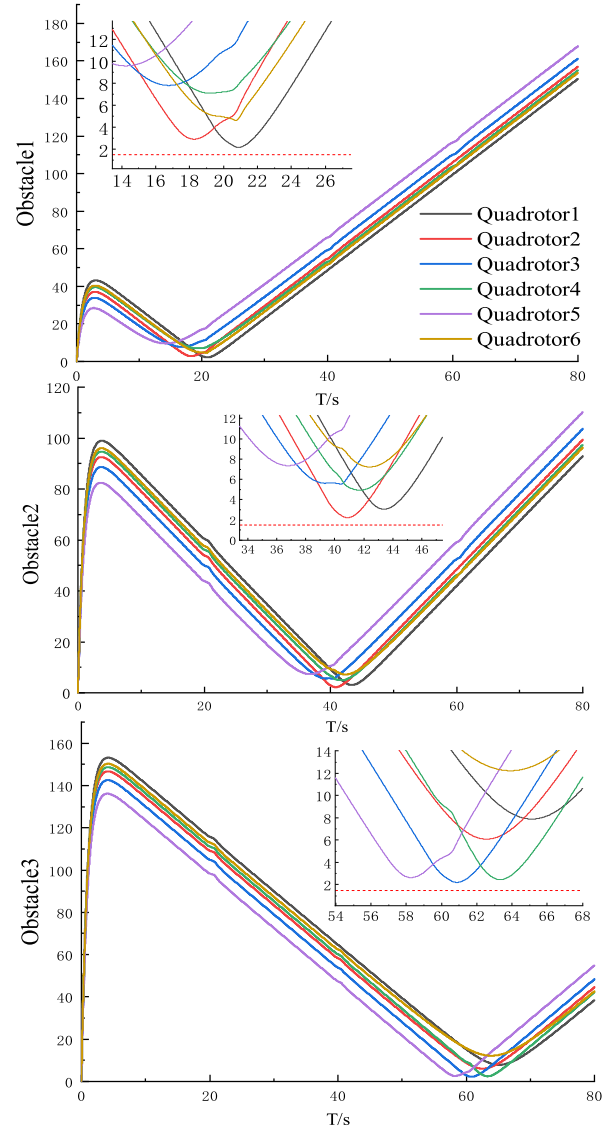

FIGURE 6. The distance between two quadrotors.

FIGURE 7. The distance between the quadrotors and the obstacles.

The proof is completed.

IV. SIMULATION

A. SIMULATION I

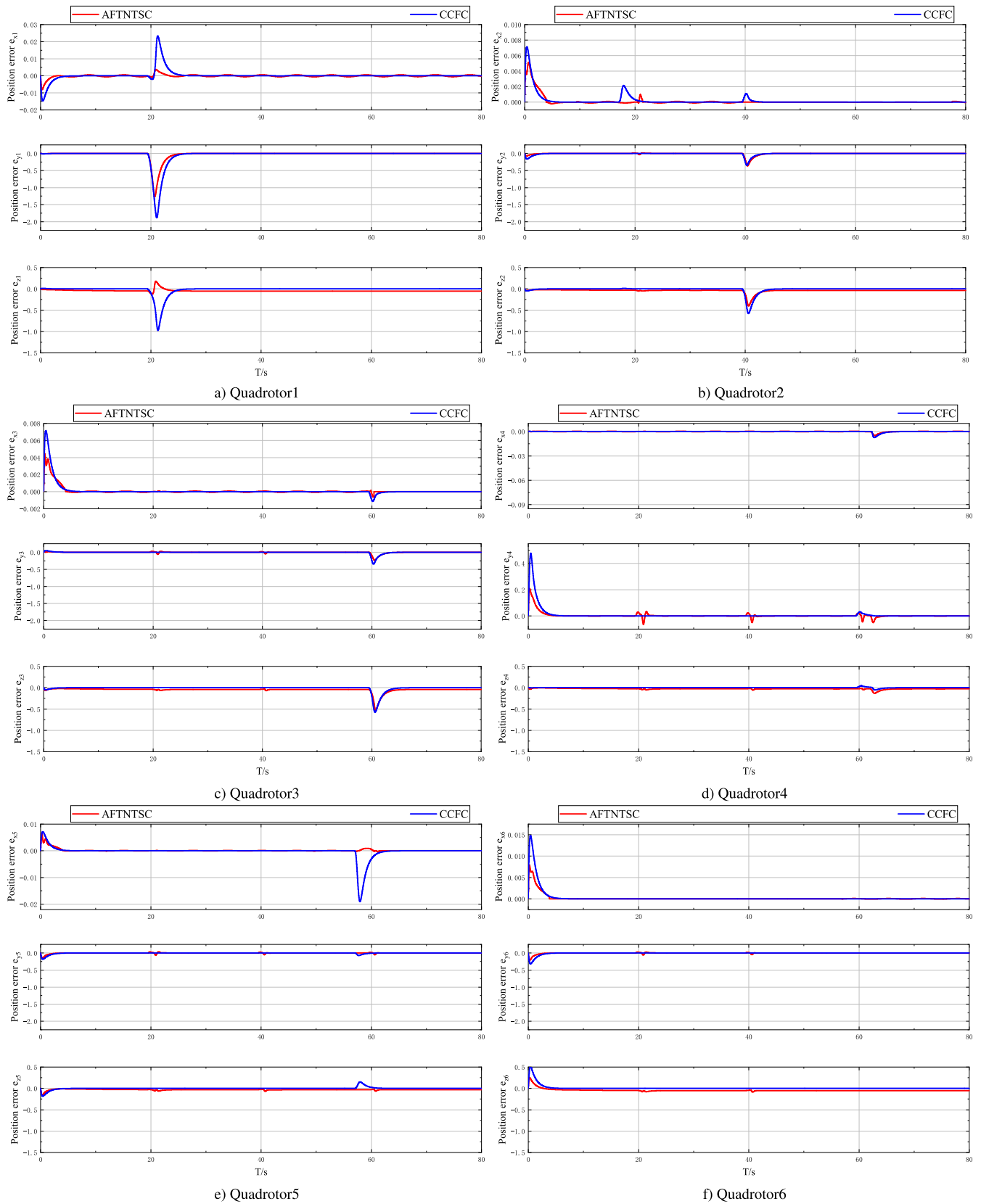For the purpose of verifying the effectiveness of AFTNTSC and the high convergence speed with a competitive tracking

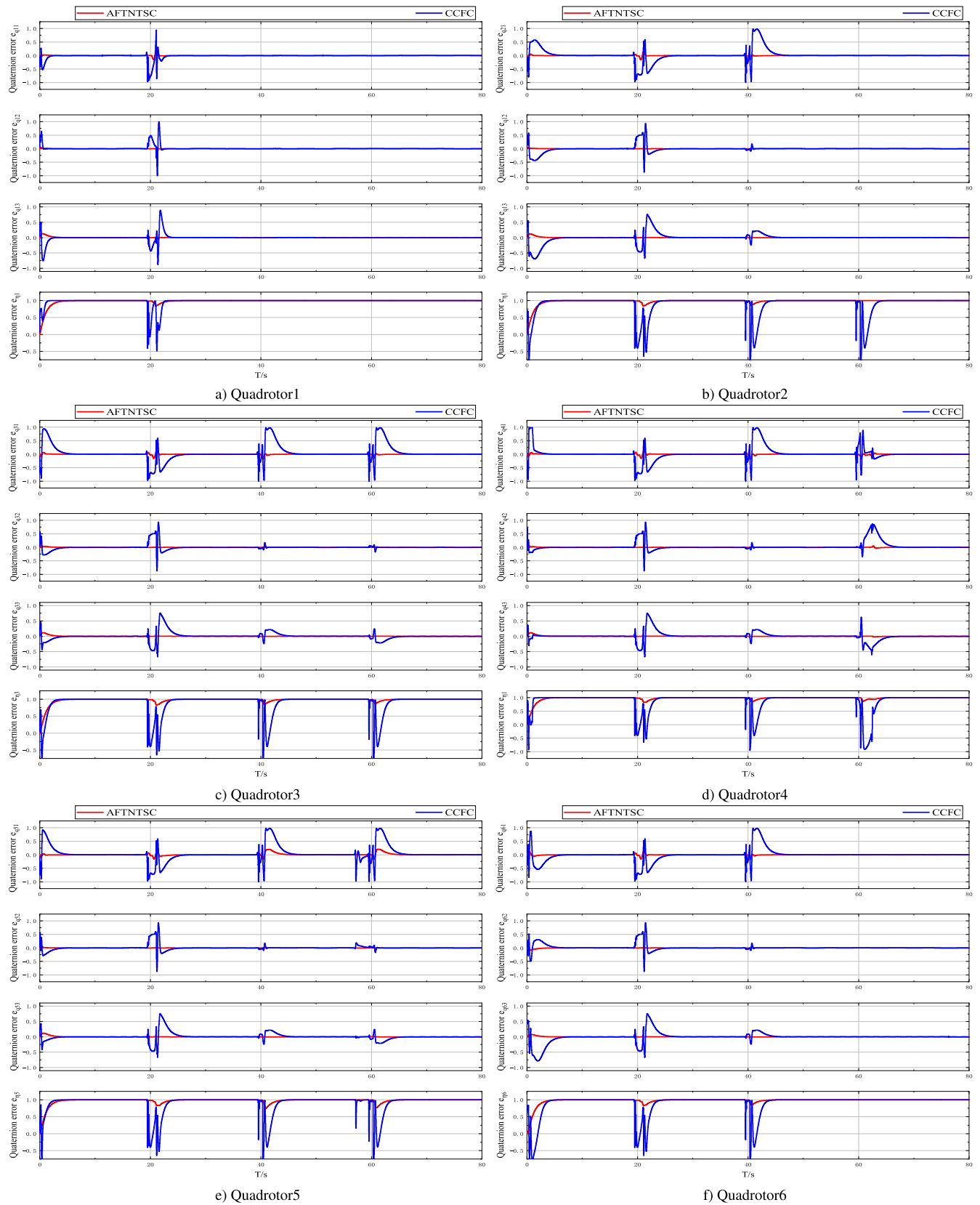**FIGURE 8.** The error function of position.
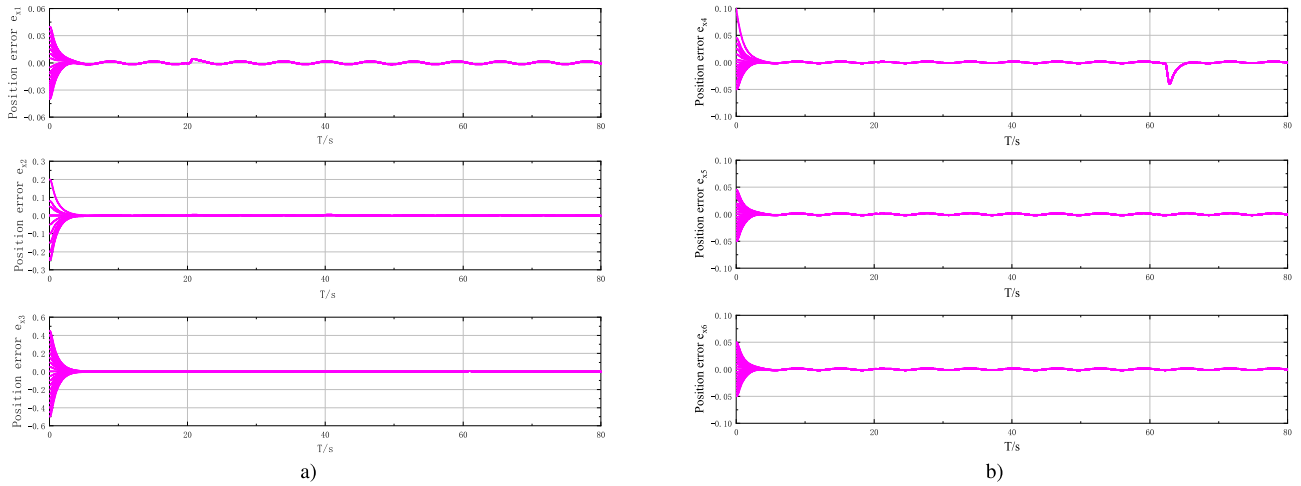
FIGURE 9. The error function of quaternion.

FIGURE 10. The error function of x_j ($j = 1,2,3,4,5,6$) in AFTNTSC.
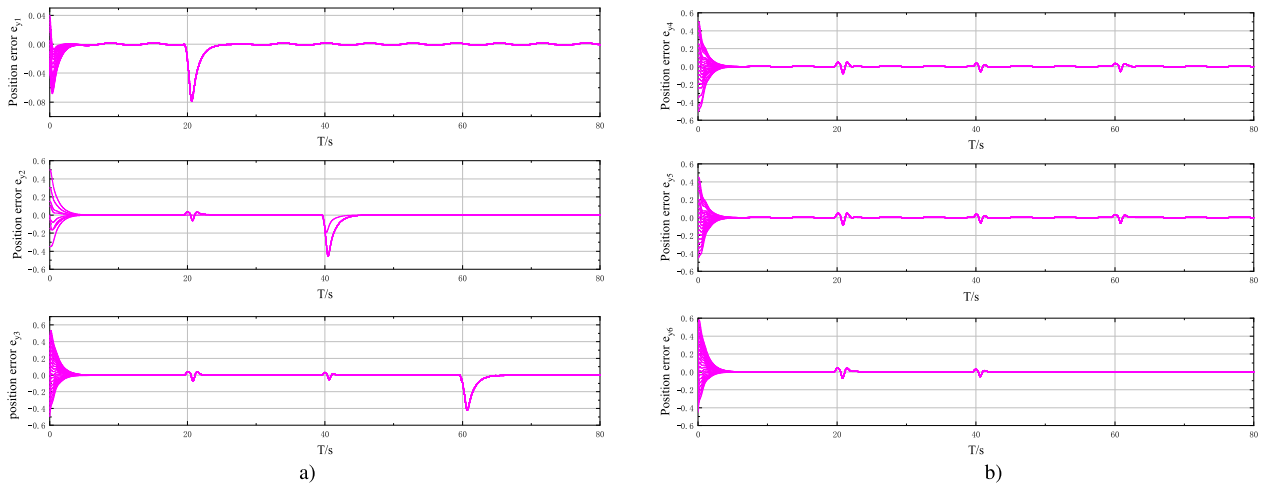

FIGURE 11. The error function of y_j ($j = 1,2,3,4,5,6$) in AFTNTSC.

accuracy, two control methods are conducted in quadrotor formation with the same initial conditions, one is AFTNTSC, and the other is consensus-based cooperative formation control (CCFC) [38]. The control law of CCFC is given as

$$\tilde{T}_{total_i}(t) = -\sum_{j=1}^{N+1} a_{ij}\left[\sum_{k=0}^{1}\gamma k(\hat{h}_i^{(k)} - \hat{h}_j^{(k)})\right],$$
$$i \in \{1, 2, \ldots, N\}$$
$$\hat{h}_j^{(k)} = h_j^{(k)} - d_{h_j}^{(k)}, \quad j \in \{1, 2, \ldots, N\}, \ k \in \{0, 1\}$$

1) PARAMETER SETTING

In this part, consider a group of six quadrotors are modeled as in (1) and (2), the structure and model parameters of each quadrotor are same. The physical parameters for each quadrotor are given as: $m_j = 1kg$, $g = 9.8m/s^2$, and the inertia matrices for quadrotor is $I_{fj} = diag\left(0.039\ 0.039\ 0.12\right) kg \bullet m^2$. d_{Uj} and $d_{\Gamma j}$ are the disturbance of the environment on the quadrotor and the uncertainty of the system model, which are

randomly considered as $d_{Uj} = \begin{bmatrix} \sin(t) & \sin(t) & \sin(t) \end{bmatrix}^T$ and $d_{\Gamma j} = \begin{bmatrix} \sin(\pi t) & \sin(\pi t) & \sin(\pi t) \end{bmatrix}^T$.

The outer-loop controller parameters are chosen as $\beta_{or} = 0.99$, $\varphi_1 = 18$, $\kappa_1 = 10$, $f_1 = \begin{bmatrix} 0.001 & 0.0015 & 0.0015 \end{bmatrix}^T$, $f_2 = \begin{bmatrix} 0.001 & 0.0015 & 0.0015 \end{bmatrix}^T$, $f_3 = \begin{bmatrix} 0.001 & 0.0015 & 0.0015 \end{bmatrix}^T$, $\Lambda_2 = 0.85$, $\iota_1 = 10$.

The inner-loop controller parameters are chosen as $\kappa_2 = 1$, $\varphi_2 = 18$, $\Lambda_3 = 0.12$, $\Lambda_4 = 0.85$, $\iota_2 = 10$, $\beta_{ir} = 0.99$. The following simulation results are obtained with $\gamma = 800$, $\lambda_1 = 5$, $\lambda_2 = 5$, $\sigma_0 = 0.5$, $r_0 = 0.5$, $\varpi = 800$, $\xi_0 = 0.01$, $R_a = 2.5$, $R_b = 1.5$, $R_c = 11$, $R_d = 8$, $R_e = 6$, $R_f = 3$, $\varepsilon_0 = 0.01$, $\varsigma_0 = 0.01$. The expected trajectory of the leader quadrotor is $q_d = \begin{bmatrix} -\frac{1}{10}\sin\frac{t}{2\pi} & \frac{5}{2}t & \frac{1}{2}t \end{bmatrix}^T$. The initial conditions of the quadrotors from 1 to 6 are chosen as $p_1 = \begin{bmatrix} -0.1 & 0.1 & 0.1 \end{bmatrix}^T$, $p_2 = \begin{bmatrix} 0.45 & 5.2 & 2.8 \end{bmatrix}^T$, $p_3 = \begin{bmatrix} 1 & 8.5 & 8.5 \end{bmatrix}^T$, $p_4 = \begin{bmatrix} 0.25 & 4.5 & 6.5 \end{bmatrix}^T$, $p_5 = \begin{bmatrix} 0.85 & 13.5 & 10.5 \end{bmatrix}^T$, $p_6 = \begin{bmatrix} 0.75 & 1.5 & -1.5 \end{bmatrix}^T$. The initial speed for each quadrotor is zero. The initial quaternion for
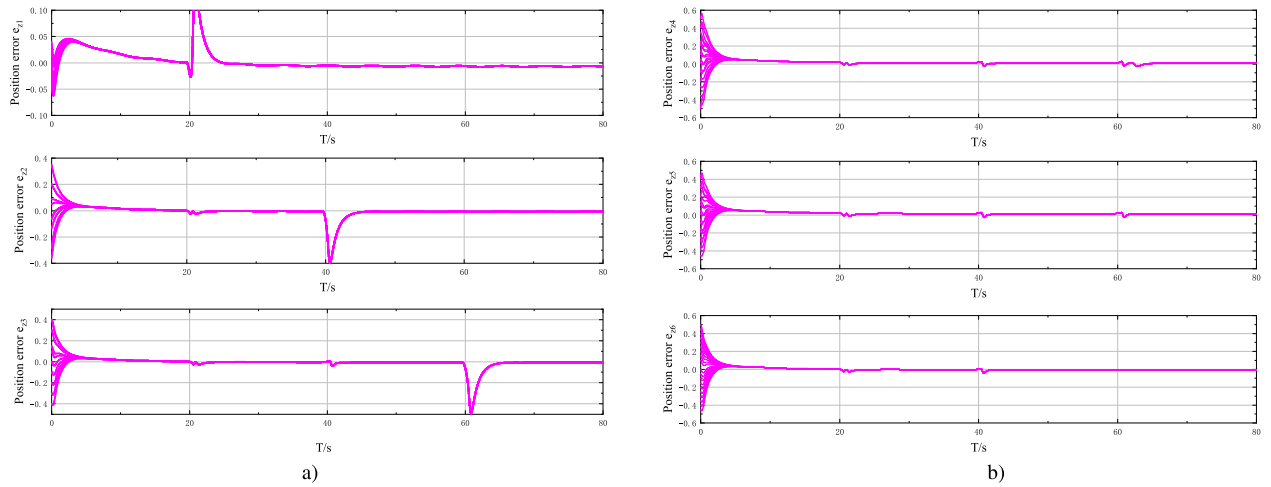
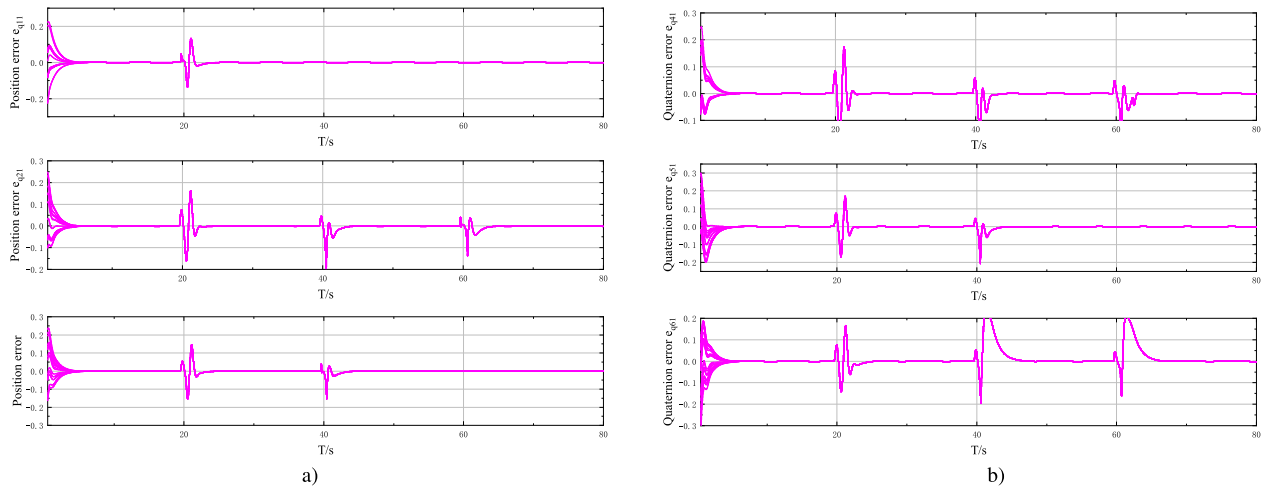**FIGURE 12.** The error function of $z_j (j = 1,2,3,4,5,6)$ in AFTNTSC.

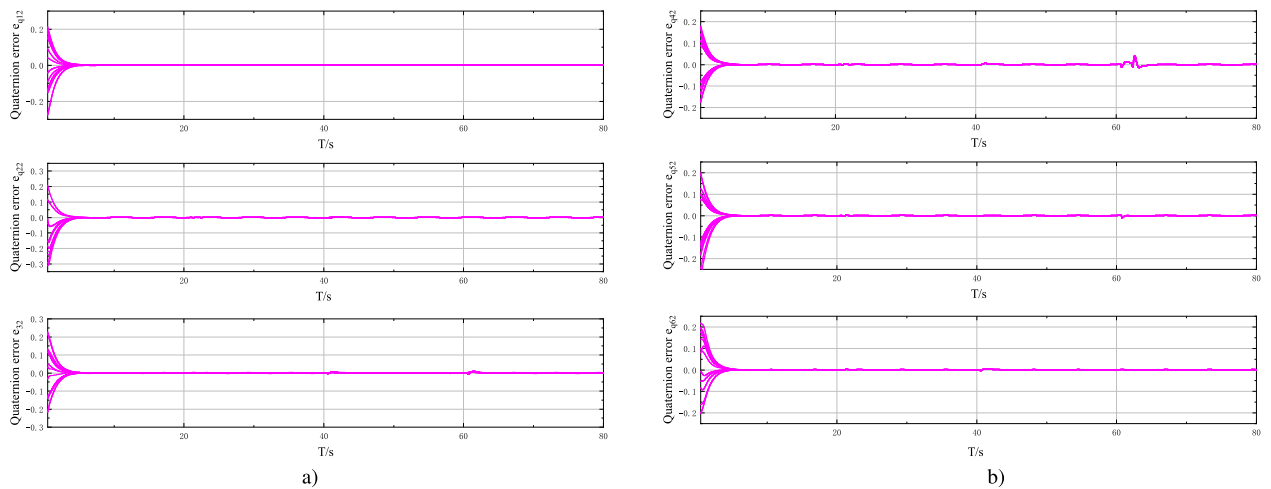**FIGURE 13.** The error function of $q_{j1} (j = 1,2,3,4,5,6)$ in AFTNTSC.

FIGURE 14. The error function of $q_{j2} (j = 1,2,3,4,5,6)$ in AFTNTSC.

each quadrotor is $Q = \begin{bmatrix} 0 & 0 & 0.6 & 0.8 \end{bmatrix}^T$, and its expectation is $Q_d = \begin{bmatrix} 0 & 0 & 0 & 1 \end{bmatrix}^T$. The initial angular velocity for each quadrotor is zero. The formation distance D

is selected as $D_1 = \begin{bmatrix} 0.5 & 6 & 3 \end{bmatrix}^T$, $D_2 = \begin{bmatrix} 0.5 & 3 & 6 \end{bmatrix}^T$, $D_3 = \begin{bmatrix} -0.75 & -6 & -2 \end{bmatrix}^T$, $D_4 = \begin{bmatrix} -0.25 & -3 & 4 \end{bmatrix}^T$, $D_5 = \begin{bmatrix} -0.2 & 6 & 3 \end{bmatrix}^T$, $D_6 = \begin{bmatrix} 0.2 & -2 & -7 \end{bmatrix}^T$, which are
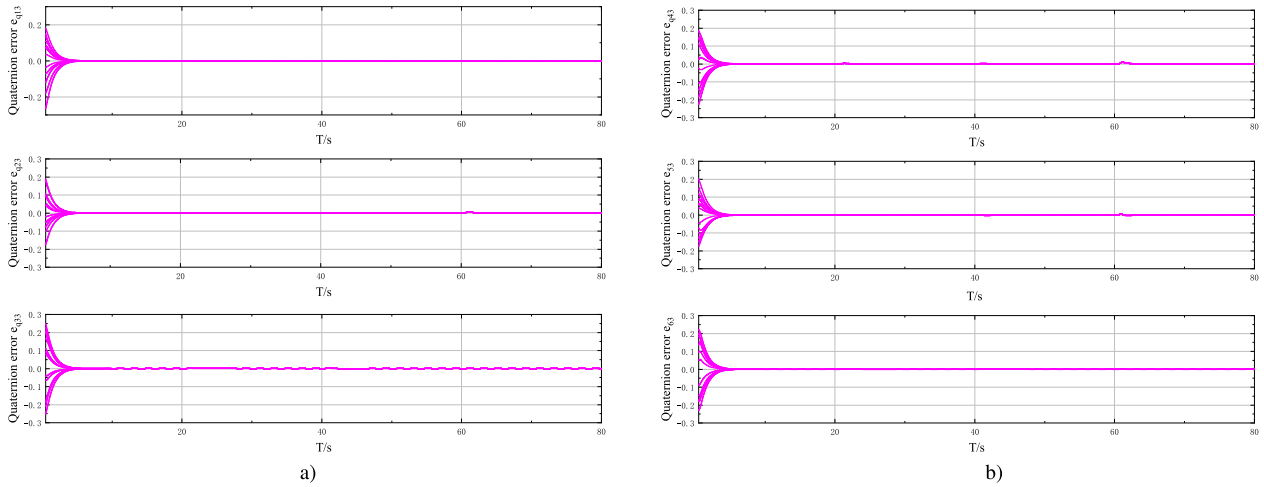
FIGURE 15. The error function of $q_{j3}(j = 1,2,3,4,5,6)$ in AFTNTSC.
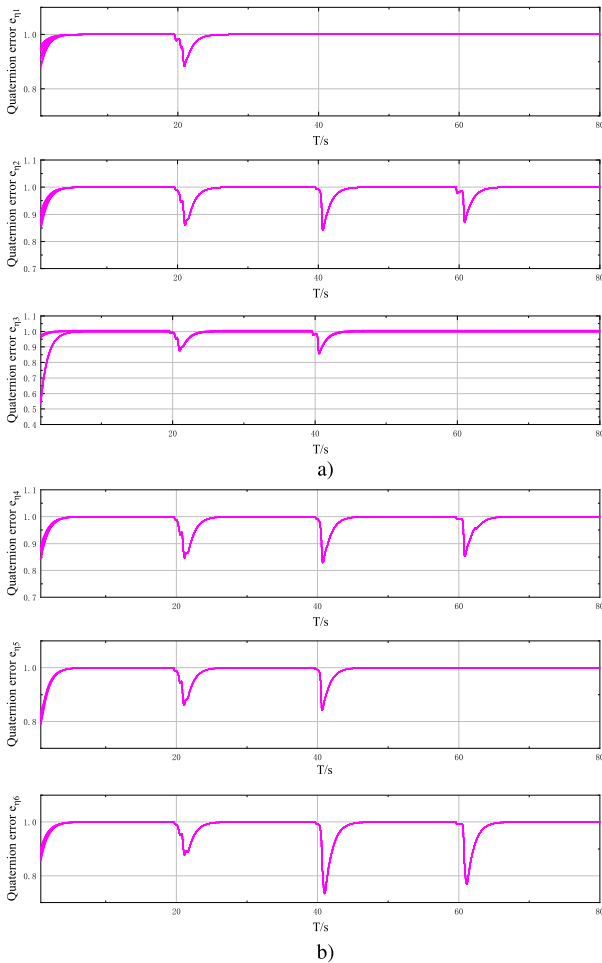

FIGURE 16. The error function of $\eta_j(j = 1,2,3,4,5,6)$ in AFTNTSC.

shown in Fig. 3. The position of the obstacles are $p_{j1} = \left[-\frac{1}{10} \sin \frac{10}{\pi} \ 50 \ 10 \right]^T$, $p_{j2} = \left[-\frac{1}{10} \sin \frac{20}{\pi} \ 106 \ 23.5 \right]^T$, $p_{j3} = \left[-\frac{1}{10} \sin \frac{30}{\pi} \ 159 \ 39.5 \right]^T$.

2) RESULTS ANALYSIS

The simulation results are shown as Fig.4-Fig.9. As is shown in Fig.4, and Fig.5, all quadrotors can track the desired trajectory and form the preset formation configuration according to the communication topology in Fig.3 with high speed. And the distance between the quadrotor and obstacle always maintain a safe distance as shown in Fig.6. From Fig.7 the two quadrotors can quickly separate and quadrotor leave obstacle in case of entering the obstacle avoidance range, and then the formation configuration is reformed. It is worth noting that in Fig.8 the fluctuation of position error of AFTNTSC is smaller than that of CCFC. It is obviously can be seen from Fig.9 that the attitude error of AFTNTSC converges faster than the error of CCFC, with small fluctuations and high convergence accuracy.

B. SIMULATION II

In order to further verify the effectiveness of AFTNTSC, Monte Carlo simulation is conducted with different initial states, and the simulation is executed 20 times. Each time the initial state is generated on $p_j = \left[x_j \pm 0.5 \ y_j \pm 0.5 \ z_j \pm 0.5 \right]^T$ and $Q_j = \left[q_{j1} \ q_{j2} \ q_{j3} \ \eta_j \right]^T$ with a uniform probability, in which $q_{j1}, q_{j2}, q_{j3} \in \left[-\frac{1}{3}, \frac{1}{3} \right]$ and $\eta_j \in \left[\sqrt{\frac{2}{3}}, 1 \right]$. Figs.10-12 show the tracking of each member of the quadrotor formation at various coordinates in multiple simulations. Figs.13-16 show the quaternion tracking of the quadrotor in multiple simulations. Figs.10-12 are the simulation result of the error function of position in AFTNTSC, and its purpose is to illustrate the advantages of this method. Figs.13-16 are the error function of quaternion in AFTNTSC. After statistics of the simulation results, a summary of these simulation results is shown in Table 1.

Remark 6: Assume that the convergence time is $x_1, x_2 \ldots x_n$ $(n = 1, 2, 3 \ldots)$. Then, the Mean convergence

TABLE 1. Statistic results of 20 simulations.

Method	Mean convergence time	Convergence time variance
AFTNTSC	4.73	0.008
FTC	5.59	0.776

time mathematical model is $\bar{x} = \dfrac{\sum\limits_{j=1}^{n} x_j}{n}$, and the Convergence

time variance's is $x_\sigma^2 = \dfrac{\sum\limits_{j=1}^{n} (x_j - \bar{x})^2}{n}$.

V. CONCLUSION

The distributed formation control problem has been investigated for quadrotor formation system with inter-quadrotor collision avoidance, obstacle avoidance and unknown disturbances. A safety control strategy and adaptive non-singularity fixed time control method have been designed for quadrotor formation. The fixed time stability of robust and safety control has been proved by Lyapunov theory. Simulation results have been demonstrated the effectiveness of the proposed formation control. In the future work, the formation control with stochastic links failure is considered.

REFERENCES

[1] D. Wang, Q. Zong, B. Tian, F. Wang, and L. Dou, "Finite-time fully distributed formation reconfiguration control for UAV helicopters," *Int. J. Robust Nonlinear Control*, vol. 28, no. 18, pp. 5943–5961, Dec. 2018.

[2] J. Wang and M. Xin, "Integrated optimal formation control of multiple unmanned aerial vehicles," *IEEE Trans. Control Syst. Technol.*, vol. 21, no. 5, pp. 1731–1744, Sep. 2013.

[3] A. Askari, M. Mortazavi, and H. A. Talebi, "UAV formation control via the virtual structure approach," *J. Aerosp. Eng.*, vol. 28, no. 1, Jan. 2015, Art. no. 04014047.

[4] Z. Ying and L. Xu, "Leader-follower formation control and obstacle avoidance of multi-robot based on artificial potential field," in *Proc. 27th Chin. Control Decis. Conf. (CCDC)*, May 2015, pp. 4355–4360, doi: 10.1109/CCDC.2015.7162695.

[5] J. Chen and Y. Xia, "Formation control and obstacles avoidance for multi-agent systems based on position estimation," in *Proc. 33rd Chin. Control Conf.*, Jul. 2014, pp. 287–296.

[6] C. Li, L. Chen, Y. Guo, and Y. Lyu, "Cooperative surrounding control with collision avoidance for networked lagrangian systems," *J. Franklin Inst.*, vol. 355, no. 12, pp. 5182–5202, Aug. 2018, doi: 10.1016/j.jfranklin.2018.04.017.

[7] Y. Cong, H. Du, Q. Jin, W. Zhu, and X. Lin, "Formation control for multiquadrotor aircraft: Connectivity preserving and collision avoidance," *Int. J. Robust Nonlinear Control*, vol. 30, no. 6, pp. 2352–2366, Apr. 2020.

[8] Y. Kuriki and T. Namerikawa, "Formation control with collision avoidance for a multi-UAV system using decentralized MPC and consensus-based control," *SICE J. Control, Meas., Syst. Integr.*, vol. 8, no. 4, pp. 285–294, Jul. 2015.

[9] V. T. Pham, N. Messai, D. H. Nguyen, and N. Manamanni, "Robust formation control under state constraints of multi-agent systems in clustered networks," *Syst. Control Lett.*, vol. 140, Jun. 2020, Art. no. 104689.

[10] Y. Huang, W. Liu, B. Li, Y. Yang, and B. Xiao, "Finite-time formation tracking control with collision avoidance for quadrotor UAVs," *J. Franklin Inst.*, vol. 357, no. 7, pp. 4034–4058, May 2020.

[11] S. Li and X. Wang, "Finite-time consensus and collision avoidance control algorithms for multiple AUVs," *Automatica*, vol. 49, no. 11, pp. 3359–3367, Nov. 2013.

[12] J. Ha and J. Shim, "An asymptotic stability involving collision and avoidance," *Korean J. Comput. Appl. Math.*, vol. 8, no. 3, pp. 605–616, Sep. 2001.

[13] X. He, Q. Wang, and Y. Hao, "Finite-time adaptive formation control for multi-agent systems with uncertainties under collision avoidance and connectivity maintenance," *Sci. China Technol. Sci.*, vol. 63, no. 11, pp. 2305–2314, 2020, doi: 10.1007/s11431-019-1528-4.

[14] J. Zhang, P. Zhang, and J. Yan, "Distributed adaptive finite-time compensation control for UAV swarm with uncertain disturbances," *IEEE Trans. Circuits Syst. I, Reg. Papers*, vol. 68, no. 2, pp. 829–841, Feb. 2021, doi: 10.1109/TCSI.2020.3034979.

[15] N. Zhang, W. Gai, M. Zhong, and J. Zhang, "A fast finite-time convergent guidance law with nonlinear disturbance observer for unmanned aerial vehicles collision avoidance," *Aerosp. Sci. Technol.*, vol. 86, pp. 204–214, Mar. 2019.

[16] H. Liu, X. Wang, X. Li, and Y. Liu, "Finite-time flocking and collision avoidance for second-order multi-agent systems," *Int. J. Syst. Sci.*, vol. 51, no. 1, pp. 102–115, Jan. 2020.

[17] J. Zhang, D. Ye, J. D. Biggs, and Z. Sun, "Finite-time relative orbit-attitude tracking control for multi-spacecraft with collision avoidance and changing network topologies," *Adv. Space Res.*, vol. 63, no. 3, pp. 1161–1175, Feb. 2019.

[18] X. Zhang, J. Gao, W. Zhang, T. Zeng, and L. Ye, "Formation control for multiple quadrotor aircraft via fixed-time consensus algorithm," *Math. Problems Eng.*, vol. 2019, pp. 1–11, Sep. 2019.

[19] J. Mao, H. R. Karimi, and Z. Xiang, "Observer-based adaptive consensus for a class of nonlinear multiagent systems," *IEEE Trans. Syst. Man Cybern. Syst.*, vol. 49, no. 9, pp. 1893–1900, Sep. 2019.

[20] Y. Sun, L. Chen, G. Ma, and C. Li, "Adaptive neural network tracking control for multiple uncertain Euler–Lagrange systems with communication delays," *J. Franklin Inst.*, vol. 354, no. 7, pp. 2677–2698, May 2017.

[21] H. L. N. N. Thanh and S. K. Hong, "Completion of collision avoidance control algorithm for multicopters based on geometrical constraints," *IEEE Access*, vol. 6, pp. 27111–27126, 2018, doi: 10.1109/ACCESS.2018.2833158.

[22] F. Yang, S. Peng, and C. C. Lim, "Neural network adaptive dynamic sliding mode formation control of multi-agent systems," *Int. J. Syst. Sci.*, vol. 51, no. 1, pp. 2025–2040, 2020.

[23] D. Wang, Q. Zong, B. Tian, S. Shao, X. Zhang, and X. Zhao, "Neural network disturbance observer-based distributed finite-time formation tracking control for multiple unmanned helicopters," *ISA Trans.*, vol. 73, pp. 208–226, Feb. 2018.

[24] Y.-Y. Chen, Y. Zhang, and Z.-Z. Wang, "An adaptive backstepping design for formation tracking motion in an unknown Eulerian specification flow-field," *J. Franklin Inst.*, vol. 354, no. 14, pp. 6217–6233, Sep. 2017.

[25] H. Liu, T. Ma, F. L. Lewis, and Y. Wan, "Robust formation control for multiple quadrotors with nonlinearities and disturbances," *IEEE Trans. Cybern.*, vol. 50, no. 4, pp. 1362–1371, Apr. 2020.

[26] X. Shao, L. Wang, J. Li, and J. Liu, "High-order ESO based output feedback dynamic surface control for quadrotors under position constraints and uncertainties," *Aerosp. Sci. Technol.*, vol. 89, pp. 288–298, Jun. 2019.

[27] L. He, X. Sun, and Y. Lin, "Distributed output-feedback formation tracking control for unmanned aerial vehicles," *Int. J. Syst. Sci.*, vol. 47, no. 16, pp. 3919–3928, Dec. 2016.

[28] D. Zhou, Z. Wang, and M. Schwager, "Agile coordination and assistive collision avoidance for quadrotor swarms using virtual structures," *IEEE Trans. Robot.*, vol. 34, no. 4, pp. 916–923, Aug. 2018, doi: 10.1109/TRO.2018.2857477.

[29] H. Pan and W. Sun, "Nonlinear output feedback finite-time control for vehicle active suspension systems," *IEEE Trans. Ind. Informat.*, vol. 15, no. 4, pp. 2073–2082, Apr. 2019, doi: 10.1109/TII.2018.2866518.

[30] H. Pan, H. Li, W. Sun, and Z. Wang, "Adaptive fault-tolerant compensation control and its application to nonlinear suspension systems," *IEEE Trans. Syst., Man, Cybern. Syst.*, vol. 50, no. 5, pp. 1766–1776, May 2020, doi: 10.1109/TSMC.2017.2785796.

[31] A.-M. Zou, K. D. Kumar, and Z.-G. Hou, "Distributed consensus control for multi-agent systems using terminal sliding mode and chebyshev neural networks," *Int. J. Robust Nonlinear Control*, vol. 23, no. 3, pp. 334–357, Feb. 2013.

[32] K. Eliker and W. Zhang, "Finite-time adaptive integral backstepping fast terminal sliding mode control application on quadrotor UAV," *Int. J. Control, Autom. Syst.*, vol. 18, no. 2, pp. 415–430, Feb. 2020.

[33] Z. Zhao, T. Li, and D. Cao, "Trajectory tracking control for quadrotor UAVs based on composite nonsingular terminal sliding mode method," in *Proc. IECON 46th Annu. Conf. IEEE Ind. Electron. Soc.*, Oct. 2020, pp. 5110–5115, doi: 10.1109/IECON43393.2020.9255196.

[34] T. Xiong, Z. Pu, and J. Yi, "Time-varying formation tracking control for multi-UAV systems with nonsingular fast terminal sliding mode," in *Proc. 32nd Youth Academic Annu. Conf. Chin. Assoc. Autom. (YAC)*, May 2017, pp. 937–942, doi: 10.1109/YAC.2017.7967544.

[35] Y. Tian, Y. Cai, and Y. Deng, "A fast nonsingular terminal sliding mode control method for nonlinear systems with fixed-time stability guarantees," *IEEE Access*, vol. 8, pp. 60444–60454, 2020, doi: 10.1109/ACCESS.2020.2980044.

[36] Z. Zuo, "Non-singular fixed-time terminal sliding mode control of non-linear systems," *IET Control Theory Appl.*, vol. 9, no. 4, pp. 545–552, Dec. 2014.

[37] C. Edwards and Y. B. Shtessel, "Adaptive continuous higher order sliding mode control," *Automatica*, vol. 65, pp. 183–190, Mar. 2016.

[38] Y. Kuriki and T. Namerikawa, "Consensus-based cooperative formation control with collision avoidance for a multi-UAV system," in *Proc. Amer. Control Conf.*, Jun. 2014, pp. 2077–2082, doi: 10.1109/ACC.2014.6858777.

DAODE ZHANG received the Ph.D. degree in mechanical and electronic engineering from the Huazhong University of Science and Technology, China, in 2012. He is currently a Professor with the Hubei University of Technology. His research interests include mechanical and electronic engineering, intelligent control, and embedded system applications.

WEI SHANG received the Ph.D. degree in aeronautical and astronautical science and technology from the Beijing Institute of Technology, China, in 2017. He is currently a Lecturer with the Hubei University of Technology. His research interests include control theory of multi-agent systems and flight control.
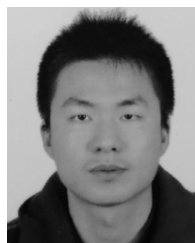
TIANLONG CHEN is currently pursuing the B.Eng. degree with the Hubei University of Technology (HBUT), Wuhan. With the help of Dr. Wei Shang, he has completed a few projects in the fields of formation control, stability analysis, and visual processing. His research interests include nonlinear control systems, nested adaptive, and trajectory tracking.

GUOHAO JING is currently pursuing the degree with the Hubei University of Technology (HBUT), Wuhan. He is currently pursuing his research under Dr. Wei Shang, and he has completed a few projects in the fields of quadrotors control, stability analysis, and data processing. His research interests include distributed control, nested adaptive, and formation control.
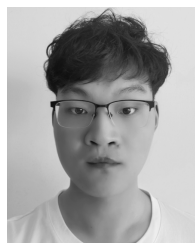
QIHANG LIANG is currently pursuing the B.Eng. degree with the Hubei University of Technology (HBUT), Wuhan. He is currently pursuing his research under Dr. Wei Shang. He has helped to complete lots of jobs of quadrotor, which include distributed control, nested adaptive, and trajectory tracking.

• • •